

University Degree in Mechanical Engineering  
2018-2019

*Bachelor Thesis*

“Manufacturing process optimization of an  
airplane wing rib by using additive  
manufacturing”

---

David Herruzo Moral

Tutora

Marta María Moure Cuadrado

Leganés, 2019



*[Include this code in case you want your Bachelor Thesis published in Open Access University Repository]*

This work is licensed under Creative Commons **Attribution – Non Commercial – Non Derivatives**



## ABSTRACT

Additive manufacturing has become one of the most growing technologies in the world in the last years, especially in industry. That is the reason why aerospace sector, which seeks to be at the forefront of technology, is implementing gradually 3D printed parts to its products.

This work looks for weight reduction of airplanes by the optimization of wing ribs manufacturing on the basis of traditional methods. This can be possible due to alternative geometries which can only be fabricated with additive manufacturing.

The proposed alternatives are ribs created by a topology optimization tool of Solid Edge software, called generative design. Based on the finite element method, this tool calculates solid parts considering given loads and constrains. Four different geometries are generated modifying their mass reduction percentage. Afterwards, the mentioned parts are 3D printed as 22 cm models at the University Carlos III of Madrid Maker Space with square and triangular filling patterns.

In order to determine the new ribs viability, their mechanical properties are evaluated by three-points bending tests in a universal testing machine at the UC3M workshop. One of the tests carried out is a rib based on typical machined ribs used as reference.

Results display a clear tendency out of generative designed ribs: rupture load and displacement increase and rigidity decreases as mass is reduced. In addition, the reference rib shows the lowest load resistance in comparison with the optimized designs and triangular filling pattern shows better performance than square pattern.

**Key words:** additive manufacturing, airplane wing rib, generative design, topology optimization.

## RESUMEN

La fabricación aditiva se ha convertido en una de las tecnologías más crecientes en el mundo en los últimos años, especialmente en la industria. Esta razón ha llevado al sector aeroespacial, que busca estar a la vanguardia de la tecnología, a implementar gradualmente piezas impresas en 3D en sus productos.

Este trabajo busca la reducción de peso de los aviones mediante la optimización de la fabricación de costillas de alas partiendo de métodos tradicionales. Esto es posible debido a geometrías alternativas que solo pueden ser fabricadas con fabricación aditiva.

Las alternativas propuestas son costillas creadas con una herramienta de optimización topológica de Solid Edge, llamada diseño generativo. Basada en el método de elementos finitos, esta herramienta calcula piezas sólidas considerando cargas y restricciones dadas. Cuatro geometrías diferentes son generadas modificando el porcentaje de reducción de masa. A continuación, las piezas mencionadas son impresas en 3D en forma de modelos de 22 cm en el Maker Space de la Universidad Carlos III de Madrid con patrones de relleno cuadrados y triangulares.

Para determinar la viabilidad de las nuevas costillas, sus propiedades mecánicas son evaluadas mediante ensayos de flexión de tres puntos en una máquina universal de ensayos en el taller de la UC3M. Uno de los ensayos realizados es una costilla basada en las clásicas costillas mecanizadas usada como referencia.

Los resultados muestran una clara tendencia en las costillas de diseño generativo: la carga y el desplazamiento de ruptura aumentan y la rigidez disminuye cuando la masa es reducida. Además, la costilla de referencia muestra la carga de ruptura más baja en comparación con las costillas optimizadas y el patrón de relleno triangular se comporta con mejor rendimiento que el cuadrado.

**Palabras clave:** fabricación aditiva, costilla de ala de avión, diseño generativo, optimización topológica.



## AGRADECIMIENTOS

*En primer lugar, quisiera agradecer a mi familia todo el apoyo que me han dado, su ánimo y su confianza durante los últimos años.*

*También agradecer a mis amigos, tanto los de siempre como los que han llegado en estos años, y a esas personas que me han acompañado y dado fuerza para continuar cada día.*

*Además, agradecer a mi tutora, Marta Moure, la oportunidad de realizar este proyecto y de descubrir el mundo de la fabricación aditiva, que tanto he disfrutado.*

*Por último, quisiera agradecer a Enrique Barbero su ayuda y su tiempo para realizar los ensayos de este trabajo, y agradecer a Carlos Cobos su trabajo y sus aportaciones a este proyecto.*

*Gracias a todos.*

## CONTENTS

1. INTRODUCTION .....	15
1.1. Motivation .....	15
1.2. Objectives .....	17
1.3. Thesis structure .....	17
2. STATE OF THE ART .....	19
2.1. Traditional manufacturing .....	19
2.1.1. Production methods .....	19
2.1.2. Joining methods .....	22
2.2. 3D printing .....	23
2.2.1. Types and materials .....	24
2.2.2. General advantages .....	29
2.2.3. Real applications on aerospace engineering .....	31
2.2.4. Aluminum 6061 on SLM .....	33
2.2.5. PLA properties for modeling .....	34
2.3. Topology optimization .....	34
2.4. Wing ribs .....	36
2.4.1. Types and materials .....	37
3. PROBLEM APPROACH .....	39
3.1. Generative designed rib .....	39
3.2. Comparison of machining and 3D printing material efficiency .....	48
3.3. Regulatory framework .....	50
4. MODELS TESTING .....	51
5. RESULTS .....	56
5.1. Individual analysis .....	56
5.2. Relative results .....	63
6. SOCIOECONOMIC ENVIRONMENT .....	67
6.1. Budget .....	67
6.2. Socioeconomic impact .....	69
7. CONCLUSIONS AND FUTURE WORK LINES .....	71
8. REFERENCES .....	73
ANEXO 1 .....	80





## FIGURES

Fig. 1.1. Evolution of materials in aviation [2] .....	15
Fig. 1.2. AM market size prediction [5] .....	16
Fig. 2.1. Wing rib machining [11] .....	20
Fig. 2.2. Stamped ribs [15] .....	21
Fig. 2.3. Riveted ribs to spar [19] .....	22
Fig. 2.4. Welded rib frame [22] .....	23
Fig. 2.5. Additive manufacturing process flow [8] .....	24
Fig. 2.6. Fused Deposition Modeling scheme [26] .....	25
Fig. 2.7. Selective Laser Melting scheme [29] .....	26
Fig. 2.8. Electron Beam Melting scheme [31] .....	26
Fig. 2.9. Stereolithography scheme [33] .....	27
Fig. 2.10. Laser Metal Deposition process [4] .....	27
Fig. 2.11. Inkjet printing scheme [34] .....	28
Fig. 2.12. Laminated Object Manufacturing draft [36] .....	28
Fig. 2.13. Pipe made in one section by AM (left) and pipe made in three sections (right) [37] .....	29
Fig. 2.14. Fuel nozzle [4] .....	30
Fig. 2.15. AM vs. traditional costs [39] .....	30
Fig. 2.16. Airbus 3D printed bracket [41] .....	31
Fig. 2.17. Conduit sections [42] .....	32
Fig. 2.18. ABS rover part [43] .....	32
Fig. 2.19. Wing rib-spar web [49] .....	35
Fig. 2.20. Topology studies results [49] .....	35
Fig. 2.21. Mass reduction level effect [51] .....	36

Fig. 2.22. Airplane wing loads [52] .....	36
Fig. 2.23. Parts of wings structure [3].....	37
Fig. 2.24. Rib loads [53].....	37
Fig. 2.25. Ribs at different locations [53] .....	38
Fig. 3.1. SC(2)-0610 airfoil.....	40
Fig. 3.2. A350 wing box section [55] .....	40
Fig. 3.3. SC(2)-0610 airfoil with rib shape .....	40
Fig. 3.4. SC(2)-0610 airfoil with generative designed rib .....	41
Fig. 3.5. Generative designed rib with loads and constrains .....	41
Fig. 3.6. Rib 1. ....	42
Fig. 3.7. Rib 2 and 3.....	42
Fig. 3.8. Rib 4. ....	42
Fig. 3.9. Rib 5, 6, 7 and 8.....	43
Fig. 3.10. Square grid filling .....	43
Fig. 3.11. Triangular grid filling.....	43
Fig. 3.12. Ribs characteristics.....	44
Fig. 3.13. Prusa i3 Mk2S [57] .....	45
Fig. 3.14. BQ PLA filament [59].....	46
Fig. 3.15. Printer and rib representation in Cura .....	46
Fig. 3.16. Printing 1 % .....	47
Fig. 3.17. Printing 10% .....	47
Fig. 3.18. Mastercam wing rib [60] .....	48
Fig. 3.19. Solid Edge rib .....	49
Fig. 3.20. Buy-to-fly ratios [61] .....	49
Fig. 4.1. Four-points bending configuration.....	52
Fig. 4.2. Three-points bending configuration.....	52

Fig. 4.3. Support parts.....	53
Fig. 4.4. Load distribution part .....	53
Fig. 4.5. Model and auxiliary parts set.....	54
Fig. 4.6. Mounted set .....	54
Fig. 4.7. Ultimaker 2 extended + .....	55
Fig. 5.1. Results rib1 .....	57
Fig. 5.2. Rib 1 after the test .....	57
Fig. 5.3. Results rib 2 .....	58
Fig. 5.4. Rib 2 after the test .....	58
Fig. 5.5. Results rib 3 .....	59
Fig. 5.6. Rib 3 after the test .....	59
Fig. 5.7. Results rib 4 .....	60
Fig. 5.8. Rib 4 after the test .....	60
Fig. 5.9. Results rib 5 .....	61
Fig. 5.10. Rib 5 after the test .....	61
Fig. 5.11. Results rib 6 .....	62
Fig. 5.12. Rib 6 after the test .....	62
Fig. 5.13. Results rib 7 .....	63
Fig. 5.14. Results rib 8 .....	63
Fig. 5.15. Mass reduction level comparison.....	64
Fig. 5.16. Filling pattern comparison.....	65
Fig. 5.17. Traditional vs. Generative designed.....	66



## TABLES

Table 2.1. Al6061 composition [45] .....	33
Table 2.2. Al6061-T6 properties [45] .....	33
Table 2.3. PLA properties [48] .....	34
Table 3.1. Ribs printing time and material .....	46
Table 4.1. Auxiliary parts printing time and material .....	54
Table 5.1. Tests results .....	64
Table 6.1. Hardware budget .....	67
Table 6.2. Software budget .....	68
Table 6.3. Material budget .....	68
Table 6.4. Energy budget .....	68
Table 6.5. Salary budget .....	69
Table A.1. NASA SC(2)-0610 Airfoil coordinates .....	80



## 1. INTRODUCTION

### 1.1. Motivation

Aerospace industry has evolved throughout its history in the direction of improvement and optimization. From early combustion alternative engines to current high-efficient turbofans, and similar evolution in materials selection, manufacturing and structures.

One of the main objectives of this industry is the continuous efficiency improvement to make air transportation cheaper and more ecologic [1]. There are two principal ways of action: more efficient engines and weight reduction.

Airplanes materials have passed through wood to metal and polymers and composites today, all of them to find a good balance among strength, light weight and low cost. Due to this progression, those flying machines have changed to get larger height, dimensions, load capacity and velocity.

Today, aerospace engineers use structural materials as high-performance alloys of steel, aluminum, titanium and other metals as well as polymers and, the greater part, composites of several types as carbon fiber with epoxy [2], illustrated in figure 1.1. Those materials are carefully selected to each application being the chosen option the lightest one with good enough mechanical properties.

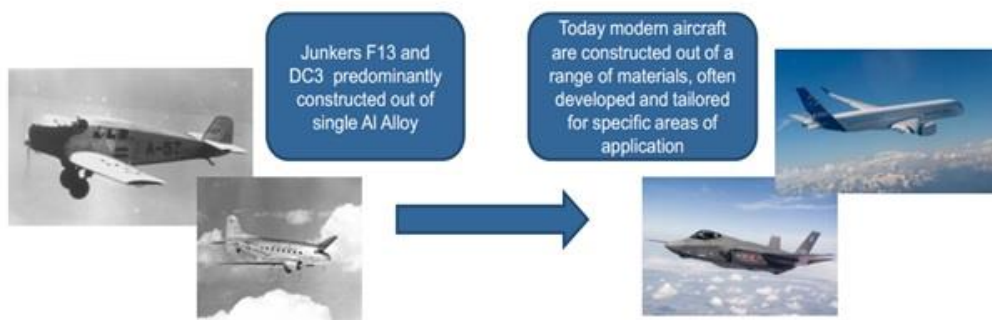


Fig. 1.1. Evolution of materials in aviation [2]

Due to this fact, aerospace manufacturers reach further limits in terms of flight range, cost efficiency, safety and environmental impact, which are sought as a sum of a lot of improvements.

One of the main structural systems in aviation are wings. They are formed by complex webs of parts to fulfill stress and flexibility requirements. Those parts are, among others,

ribs, spars, stringers and skin. Ribs are in charge of transmitting loads from outside (skin) to inside (spars), creating wing boxes. Skin, reinforced with stringers, and spars form the longitudinal walls of the boxes and ribs provide rigidity transversely [3]. The importance of rib is crucial but there are so many of them that it is important to keep them under weight restrictions.

Manufacturing methods are other line of optimization to build more efficient structures with less elements and mass but the same strength and a restrained outlay. That reason explains the appearance of technologies such as laser welding and powder-metal parts [2], but there exist other manufacturing improvements trying to become noticeable like additive manufacturing (AM).

AM is an alternative manufacturing method to traditional methods. It is awaking interest due to its numerous advantages such as no geometry restrictions, what make possible internal cavities, inner patterns instead of solid bodies and organic-like shapes, all of them for the sake of optimized structures and lightening [4].

Smart Tech Publishing [5] has analyzed the tendency of additive manufacturing in the last five years and predicted it for the next eight year, as shown in figure 1.2. The market size for professional sector has been multiplied by almost three times from 2014 and will presumably continue growing to ten times its value by 2027. That makes investments in AM to be profitable for the short and large term.

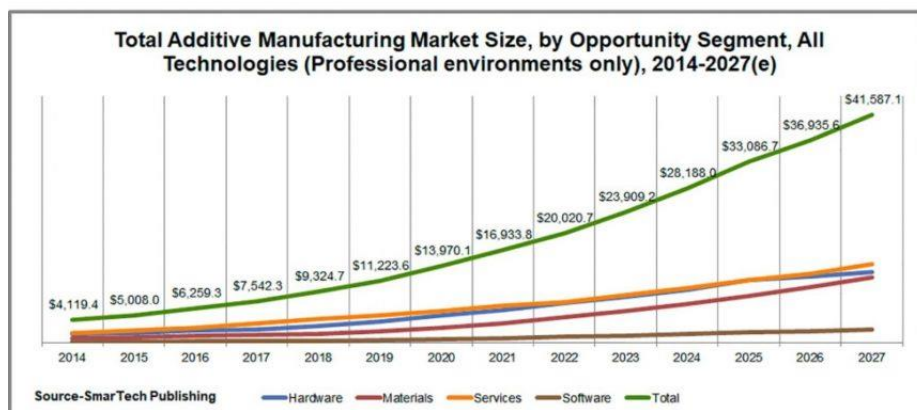


**Fig. 1.2. AM market size prediction [5]**

In this work, some real applications and solutions are shown. However, most of them are restricted to small parts which helps to improve cost effectiveness proportionally. If those advantages are taken to large scale parts, the benefit for airline companies and for customers could result very significant. With the help of generative design and 3D printing technologies, it will be evaluated the possibility to optimize airplanes wing ribs,



considering that small individual weight reduction means very influent regarding the high presence of them in an airplane. This is possible using topology optimization tools like Solid Edge and additive manufacturing, which is the only way to build the new generated structures.

## **1.2. Objectives**

The main objective of this work is to perform an optimization processes over a wing rib by using Additive Manufacturing processes instead of using traditional manufacturing processes. To achieve this main goal, four secondary objectives must be fulfilled:

- Evaluate additive manufacturing benefits in comparison with traditional manufacturing. This goal may be achieved during the development of the work concerning aspects such as time, cost, effectiveness and ease of work, which are characteristics of rapid prototyping, for instance.
- Design different alternatives of wing rib scaled models developed by means of generative design tools and 3D printing technology.
- Carry out experimental tests on the designs previously developed. Analysis of the new geometries from the results of different bending tests including a traditional rib design for contrast.
- Carry out and optimization process by means of the observation of the influence of some generative design and 3D printing parameters (infill percentage, filling pattern or generative study accuracy) in terms of weight, cost and strength. The use of those automated technologies makes easier to combine different settings and evaluate the best options.

With the results obtained in this work for the wing rib, the same procedure could be applied in other components of aerospace industry and also in other sectors such as automobile industry.

## **1.3. Thesis structure**

This work is developed converging from the theory basis related with the two main issues in question, 3D printing and wing ribs structure, to the test's results analysis. It is divided into six chapters, not including the introduction:

- State of the art: it gathers all the necessary theory for the proper development of the problem solution. First, the main features of traditional and additive manufacturing are described, with their methods, materials, benefits and

disadvantages. Second, it is described the method of topology optimization and generative design and finally the functioning of wing ribs and their load demand.

- Problem approach: this chapter comprises the whole procedure of designing and printing of the rib models, that is, from the NACA profile of a wing to the use of generative design tools, and last, the steps and setting to properly built all the parts. Also, it includes the regulatory framework.
- Models testing: the tests are the practical part of this work. They are explained to justify how they are adapted as far as possible to the loads and constraints required.
- Results: after the tests, the results are expressed in different graphs, individually and relatively among them.
- Socioeconomic environment: it is formed by the project budget and socioeconomic impact. The budget is broken down in the different expenses categories and the socioeconomic impact takes into account all the possible changes that this project and its future development could done into society.
- Conclusions and future works: at the end, the results are analyzed and put together to find a resolution with their positive and negative aspects. Also, it is added a list of possible work lines to complement this work.

## 2. STATE OF THE ART

It is necessary to compare traditional manufacturing methods with 3D printing, to understand the advantages and disadvantages of the latter, thus, a brief evaluation of the principal manufacturing methods used in wing rib production is presented. With the aim of working with 3D printed wing ribs, two different technologies need to be considered and join them together. First of all, additive manufacturing (AM), its variants and applications. Then, wing ribs, their types and the working conditions to which they are subject.

### 2.1. Traditional manufacturing

Depending on loads and costs constraints, most planes are implemented with forged or machined ribs for high stress demand [6] but there are other options as stamped ribs for lower loads or truss ribs, used mainly for small airplanes because of its simplicity and cost [3]. Those production processes and the principal joining methods used in that industry are described and listed some benefits and disadvantages applied to aircrafts construction.

#### 2.1.1. Production methods

##### Machining

Machining includes all process which removes material by a machine tool on different materials like metals, plastics or wood. Some of those processes are drilling, milling, grinding or turning using, among others, drilling centers, milling centers or lathes and numeric controlled machines like CNC lathes or machining centers. Those processes need cutting consumable edges like drill bits or machining inserts.

CNC Machining is a type of computer-aided manufacturing that needs a software and a hardware able to reproduce it. The software used manages a program written, generally, in G-code language that makes a series of tools to work on the working material to obtain the exact geometry preset.

It is full autonomous so, after the program is written, no human action is required. Thus, the products are true copies of each other. Also, CNC machining can be a cheap manufacturing solution since it does not need the job of skilled workers during the shaping operation. The high investment made on the machine can be eventually amortized due to this fact.

Another advantage is time saving. Machining sets can be optimized and kept for the rest of works, needing only a G-code to start the operation [7].

On the contrary, a big amount of material is wasted, and geometry limitations depends on the tools working axis and on the geometry of the final product in comparison with other methods [8].

For the aerospace industry, the technology used is CNC as very precise geometries are needed out of computer assisted designs. It also needs a combination of large parts and CNC machined parts for which specific extra-sized machining centers have been created [9] like the one showed in figure 2.1. The use of superalloys in aerospace is another difficulty solved with special machining techniques [10].

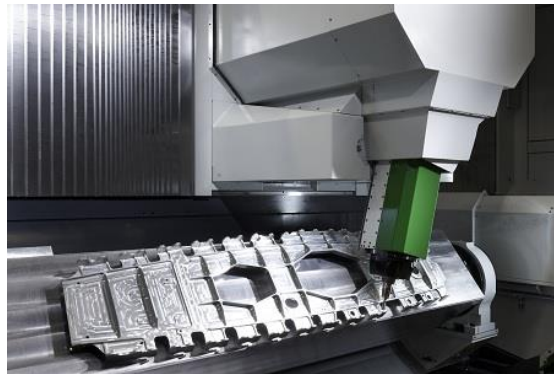


**Fig. 2.1. Wing rib machining [11]**

### Stamping

Metal stamping includes a wide variety of process like blanking, piercing, bending, deep drawing or punching [12]. For wing rib several forming processes take place: bending, piercing, blanking and shearing [13].

Those operations can be done by hand with a series of manual tools, patterns and dies or by a press with a set of punches and dies, progressively or in a single punch [12].

To manufacture ribs like the ones in figure 2.2, first the external shape of the part is blanked on a sheet metal. After that, riveting holes are drilled or pierced, and lightening holes can be cut or punched too. Finally, bending operations are performed at the edges, for later joining with spars and skin, and on specific locations to create stiffening protuberances [13].

Stamping is considered one of the cheapest manufacturing methods due to the good repeatability for high volume batches very fast and low human interaction. Also, stamped parts can be made with high precision. Those benefits are possible thanks to specific tooling for a single part design attached to automated machinery.

Although, if production volume is under a certain number of parts, that specific tools and dies are very costly to create and lead time augments as it must be design and fabricated [14]. In addition, parts are limited to constant thickness plates with few possibilities in the out-of-plane direction.



Fig. 2.2. Stamped ribs [15]

### Forging

The process of forging consists of the plastic deformation of a piece of metal, like a billet, by the pressure of two dies against each other. Metal is in solid state but heated until a different temperature depending on the type of forge. It could be performed into a close or an open die and in one or several punches, called progressive forging. Forged parts show better mechanical behavior than other methods. Moreover, it represents one of the most cost-effective manufacturing processes for large and medium production volumes because of the use of the same dies for all the batch and the percentage of scrap is very low in comparison with machining [16].

However, these advantages also lead for a worse flexibility and the need of expensive specific tooling only amortized over a certain quantity of production, similar to stamping. Parts geometry is also limited by the metal viscosity so it can flow easily through the die cavities without letting them empty, which is one of the most common failures [16]. Another disadvantage is the lack of finishing quality so it might need further processes to assure accurate dimensions or smooth surface [17].

Forged parts are high strength components used for mechanical applications. In the case of forged ribs, they are reserved for high load demand zones in the wing [17].

### 2.1.2. Joining methods

It is well known that the fuselage of an aircraft is not a monolithic piece. During its manufacturing process several structural elements need to be joined with mechanical, adhesive or welded joints. [18].

#### Riveting

Mechanical joining is the most used because of reliability and maintenance simplicity and is implemented by rivets, bolts or fasteners [18], being riveting the method seen in ribs, spars and skin.

Using traditional manufacturing procedures, most ribs are manufactured by machining or stamping [6] and, in the case they are composed by several parts, those parts need to be riveted. Therefore, the joining lines or areas are full of thousands of riveting holes. This fact can represent an important issue as each hole acts as a load concentration spot [18].

For instance, the rib shown in figure 2.3 has riveting holes prepared for the union with the skin, and other already riveted with other parts and with one of the spars. Later in this chapter, alternative manufacturing processes will be proposed to avoid some of these holes.



**Fig. 2.3. Riveted ribs to spar [19]**

#### Welding

Some planes and helicopters are built using a truss frame (see figure 2.4) including its fuselage and the wings structure [20]. This frame is formed by a number of tubular steel



bars welded among each other. Truss ribs are the most lightweight and load efficient type, although the most difficult to construct [3].

Welding can be applied to almost all types of metals, thermoplastics and some ceramics. Welding areas can surpass the strength of substrate eliminating stress concentrations and it can be done with high precision automated systems to assure maximum quality, crucial for structural standards in aerospace.

On the other hand, disassembly is restricted or impossible in welded joints, what makes it unviable for parts suitable to be substituted. Also, the heat affected zone about the weld beam can negatively affect the microstructure of the substrate making it to lose mechanical properties and create residual stresses too. Finally, for specialized jobs as the constructions of airplane structures, qualified professionals or complex automated systems can make welding very costly [21].

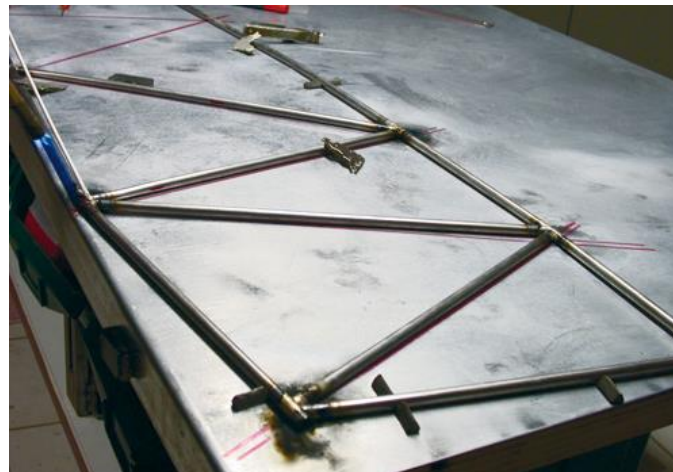


Fig. 2.4. Welded rib frame [22]

## 2.2. 3D printing

Additive manufacturing or 3D printing is the technology able to create objects adding material from zero. It makes volumes adding material layer by layer and bonding each layer to the previous one [8]. Hence, any internal and external structure can be constructed from a CAD object and an AM printer following the process described in figure 2.5.

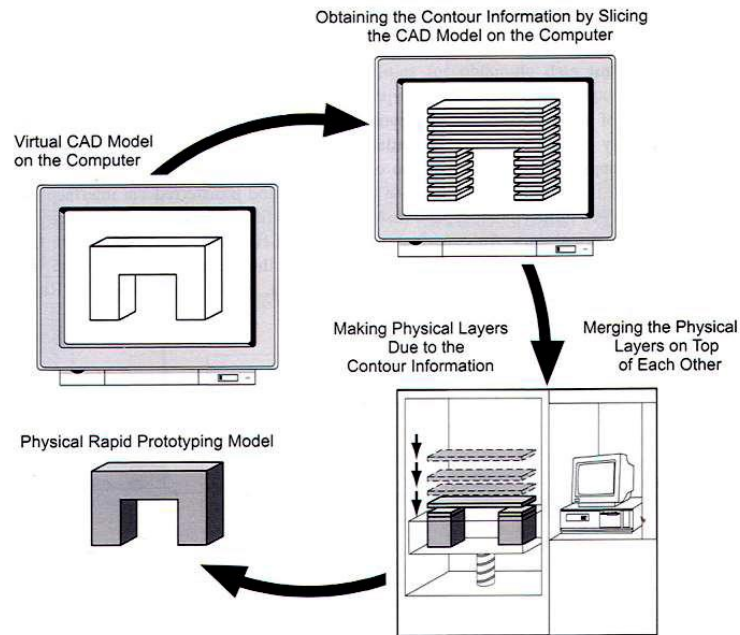


Fig. 2.5. Additive manufacturing process flow [8]

### 2.2.1. Types and materials

There exist several AM methods, each of them works with one or more materials. Some uses plastic polymer powder or filaments, metal powder, ceramics or even composite materials [8]. The following lines describe the most common processes, the different materials used by them and some of their advantages and drawbacks. They could be classified by their type as material extrusion (FDM), powder bed fusion (SLS, SLM, EBM), photopolymerization (SLA), laser metal deposition (LMD) [23], inkjet printing and laminated object manufacturing [24]:

- **Fused deposition modeling (FDM):** a thermoplastic polymer filament is heated to approximately  $2^{\circ}\text{C}$  above its fusion point and passed through a nozzle [8]. The fused filament is deposited on a working surface and then layer upon layer (see figure 2.6) with a typical thickness of  $200\text{ }\mu\text{m}$  [25]. The polymer solidifies almost instantly at room temperature.

The most common materials are polycarbonate (PC) and acrylonitrile butadiene styrene (ABS) but some manufacturers also uses polylactic acid (PLA), nylon and polymers reinforced with fibers or metals [23, 24].



This method provides cost-effective, high speed prototypes and functional parts for low stressful tasks. However, surface quality and mechanical properties are limited and depends on layers width, thickness and direction [24].

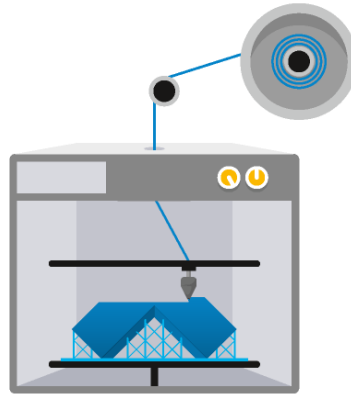


Fig. 2.6. Fused Deposition Modeling scheme [26]

- Selective laser sintering (SLS): plastic, metal or ceramic powder packed on a container is deposited on very thin layers (most common 100  $\mu\text{m}$  [25]) and sintered by a laser beam with the shape of the cross-section area at each layer. The material is already heated until nearly its melting point to facilitate the process [8].

A wide variety of materials can be laser sintered like metals, polymers, ceramics and combinations between metals and the other two [8].

SLS obtains high quality and complex geometries, also it does not need support structures since powder acts like support. On the contrary, as powder is not fully melted, parts presents porosity and hence bad mechanical properties [8].

- Selective laser melting (SLM): a process similar to SLS. This time the material is fully fused by a high energy laser beam (see figure 2.7) in a modified atmosphere and layer thickness is about 100-250  $\mu\text{m}$  [27]. The material solidifies rapidly to form well-defined parts with less porosity than sintered ones [28].

Aluminum, nickel, iron, titanium, copper, magnesium among others and their alloys [28] or even metal-ceramic compounds [27] are suitable for SLM.

Complex parts with significantly well mechanical properties, due to a uniform microstructure, are the products of that process. As its main disadvantage, residual stresses after solidification lead to not enough dimensional accuracy for some industries [28].

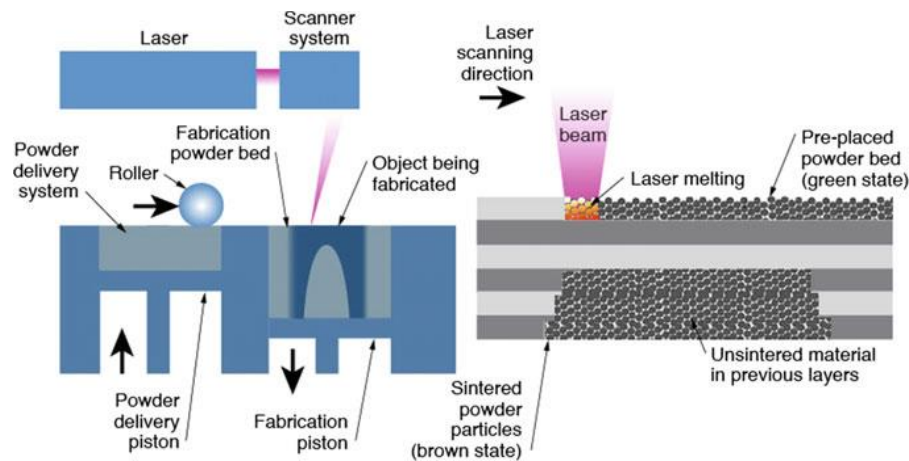


Fig. 2.7. Selective Laser Melting scheme [29]

- Electron beam melting (EBM): as other powder bed methods, metallic powder is deposited layer upon layer. EBM uses as energy source a beam of electrons instead of photons, as seen in figure 2.8.

The process needs a vacuum atmosphere, which lets high speed scanning up to  $10^5$  m/s, but there exists an electrostatic charge danger. On the other hand, materials are very restricted, only electron conductive materials can be used so electrons can flow between particles [30].

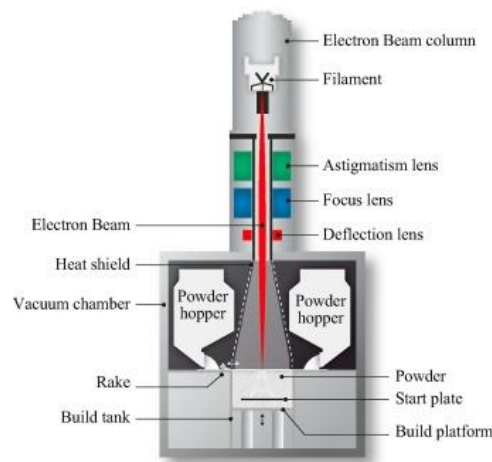


Fig. 2.8. Electron Beam Melting scheme [31]

- Stereolithography (SLA): SLA is based on the photo-polymerization of liquid resin by UV light. The construction is made layer by layer being the layer thickness the distance between the working part and the liquid surface, like in figure 2.9, or bottom, depending on the apparatus type. Most commonly  $50\ \mu\text{m}$  [25].

It can achieve a very high resolution up to 20  $\mu\text{m}$  details. In the case of some materials, post-processing light treatments are required to improve mechanical properties as some monomers remain unpolymerized [32].

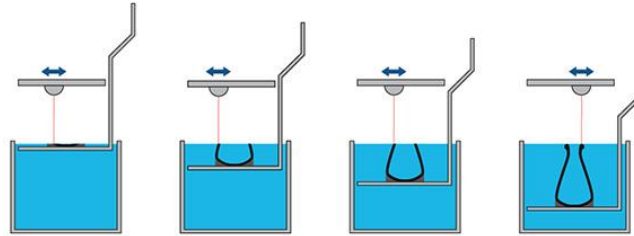


Fig. 2.9. Stereolithography scheme [33]

- Laser metal deposition (LMD): [24] known as the most popular direct metal deposition method, consisting of the union of an energy source, like a laser beam, and projected powder metal against a particular small area. The laser both melts the substrate and the new material and forms the new shape layer by layer. This process is exposed in figure 2.10.

Materials like titanium, aluminum, stainless steel and their alloys are some of the possible list. This and similar AM types are highly useful for repairing works on medium and large metal parts.

LENS is relatively fast, 0.5 kg/h deposited, and provides good mechanical properties [24]. However, compared with powder bed fusion technologies, parts geometry needs to be fewer complex and surface may require post-processing machining for better finishing [8].

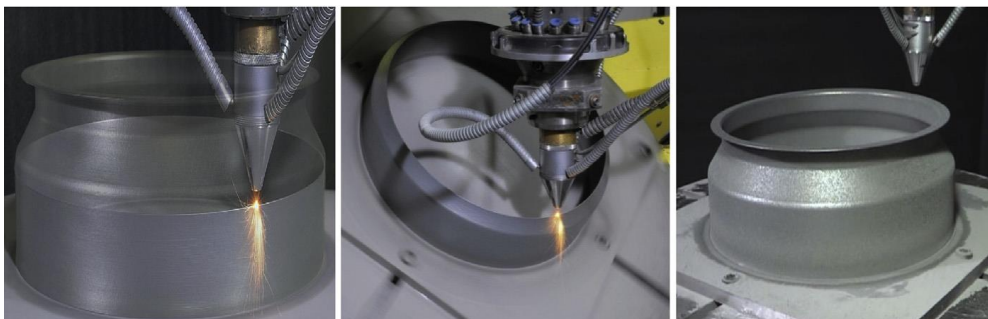


Fig. 2.10. Laser Metal Deposition process [4]

- Inkjet printing [24] could be considered another powder bed fusion but this time two components form the final material. Ceramic or metal powder is bonded layer

by layer by wax-based ink, as if it was a 2D printer. Once a layer is completed, a new powder layer is deposited by a roller, illustrated in figure 2.11.

Coarse finishing but fast and efficient manufacturing makes this method suitable for modeling and prototyping.

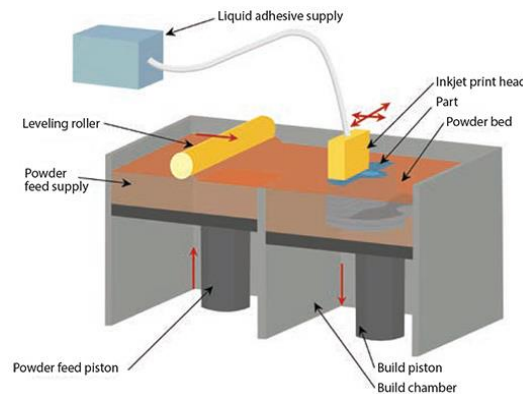


Fig. 2.11. Inkjet printing scheme [34]

- Laminated object manufacturing (LOM): for the construction of each layer a thin sheet is placed, cut by a laser or cutter and bonded to the previous layer, with an adhesive element between them (see figure 2.12). Bonding needs pressure and heat to enhance the union and avoid bubbles [35]. Different materials like paper, thermoplastic or metals are suitable for bonding.

LOM is a good option when large or low-cost structures are required. However, for accurate dimensions and good surface finishing it needs post manufacturing processing, which increases the cost. Also, bubbles and overheating can produce defective adhesion between layers [24, 35].

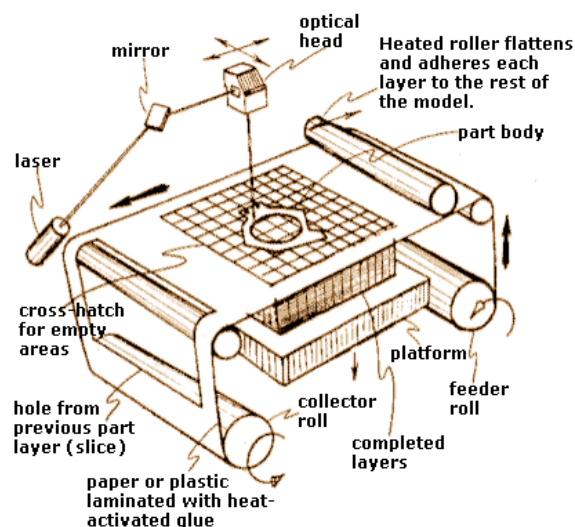


Fig. 2.12. Laminated Object Manufacturing draft [36]

Out of this list and taking into account the advantages and disadvantages of each element, the most suitable methods for this project are FDM for manufacturing the test models and SLM to describe theoretically the real manufacturing process for the final rib.

### 2.2.2. General advantages

Most advantages that AM can provide are not only translated into time and cost savings but also into performance improvements.

Compared with traditional manufacturing processes characteristics [8]:

- Material saving: AM spends just the amount of material needed, whichever the material is. In case of the existence of leftovers, as powder bed fusion or SLA cases, they can be used again.
- Resource simplicity: no extra tooling is needed, only the 3D printer and the material. This eliminates consumable items as cutting tools or lubricants.
- Design flexibility: There is no geometry limitation apart from size. Innovative and complex functions can be implemented on designs from the CAD model without taking into account the tools available. Moreover, parts can be manufactured in a single piece without the need of any type of joint caused by geometry constraints. As shown in fig. 2.13, the pipe on the right could not be manufactured in one part by traditional methods and the fuel nozzle appearing in fig. 2.14 has been optimized from 18 parts to only 1 and 25% of weight reduced [4].



**Fig. 2.13. Pipe made in one section by AM (left) and pipe made in three sections (right) [37]**



**Fig. 2.14. Fuel nozzle [4]**

- As no molds are required, designs can be modified in any phase of the project without any extra cost.
- Less human interaction, hence less errors. Final part quality only depends on the designer abilities, who does not need manufacturing knowledge.
- Batch cost: it costs the same to produce 100 different customized parts as 100 identical parts [38] and it is also independent from the manufacturing volume as shown in fig. 2.15.

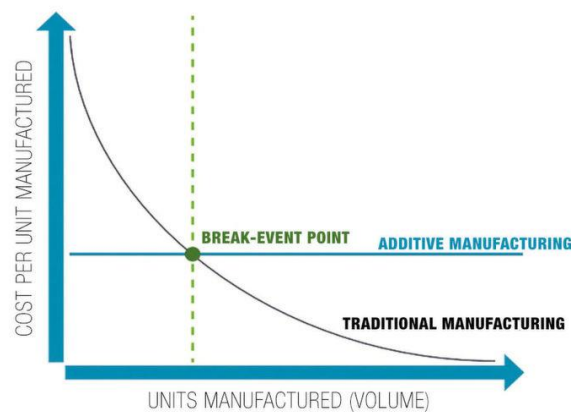


**Fig. 2.15. AM vs. traditional costs [39]**

Rapid prototyping and modeling [8]:

- Faster iteration of designs, errors can be corrected directly in the CAD document and produce a new prototype in a very short time.

- Models can be tested on the final assembly before producing the final part. That is especially helpful if the final part production needs to be expensive and time-consuming.

Another good application for AM is rapid tooling. Tools and jigs are typical on demand objects in industry and they are usually ordered to external partners as they could be not manufactured by the company which need them. Then a big part of the annual budget is spent on those utensils.

To optimize tooling costs Volkswagen uses Ultimaker 3D printers for jigs and fixtures production so they can design and obtain one of these parts every time a new project starts with a lead time close to zero, compared with their old external manufacturers ordering procedure [40].

### 2.2.3. Real applications on aerospace engineering

Functional parts are possible to be built too, depending on the application stress demand. There exist some companies using additive manufacturing which have been stated before and others, specially applied to aerospace, like Airbus or Stratasys.

Airbus [41] has implemented for the first time a 3D printed part on one of their production airplanes. It is a titanium bracket for the A350 engine pylons. The reason why they decided to start using additive manufactured parts is that they can present lower static forces and less fatigue than conventional machined parts.

As it is seen in fig. 2.16, AM technologies enables the production of this bracket with internal complex geometries or even hollow section, both unattainable for a milling head.

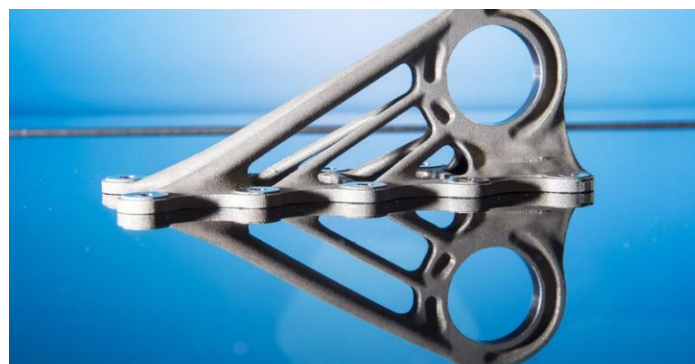


**Fig. 2.16. Airbus 3D printed bracket [41]**

Stratasys shows two projects benefited from their 3D printing advantages: quality prototypes for Bell Helicopter [42] and NASA's light rover parts [43].



Bell used printed branched conduits prototypes (see fig. 2.17) for fitting testing on the Osprey helicopter. They tried 42 models to find the optimum design in just 2 days and a half, against six weeks that it would have taken to manufacture them in aluminum. Those prototypes were made in polycarbonate, a material which stands impacts and chemicals, and modeled by FDM, which is one of the most affordable and fast method for rapid prototyping

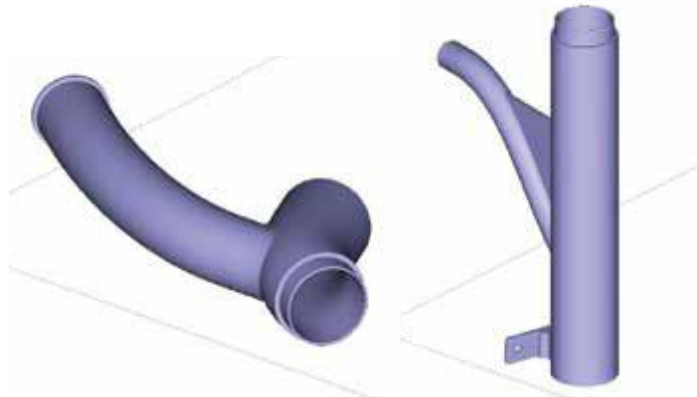


**Fig. 2.17. Conduit sections [42]**

The second example is a human transporting rover developed by NASA. It should support very hard conditions and a pressurized cabin, so it requires the most accurate and light parts. Approximately 70 pieces for this project were taken directly from digital designs of specialized electronic assemblies, vents, housings, tailored fixtures (as the one in fig. 2.18) among others made of different thermoplastics. Parts are FDM modeled since they need to be as lightweight and strong as possible but also manufacturable and affordable, no extra tooling.



**Fig. 2.18. ABS rover part [43]**



#### 2.2.4. Aluminum 6061 on SLM

Al6061 is one of the most used materials in aerospace due to its mechanical properties and its machinability. It needs thermal treatments to reach the best strength properties, most likely T6 treatment: separate solution treatment, rapid quenching and artificial ageing [44]. It is formed by aluminum and several precipitant metals gathered in table 2.1 and its properties in table 2.2.

**Table 2.1. Al6061 composition [45]**

	Cu	Mg	Zn	Mn	Si	Fe	Cr	Ti
Weight %	0.15–0.4	0.8–1.2	0.25max	0.15max	0.4–0.8	0.7max	0.04–0.35	0.15max

**Table 2.2. Al6061-T6 properties [45]**

Density	2.7 g/cm <sup>3</sup>
Ultimate Tensile Strength	310 MPa
Tensile Yield Strength	276 Mpa
Modulus of Elasticity	68.9 Gpa

Due to those properties, Al6061 is also demanded in additive manufacturing industry, especially for selective laser sintering and melting. Despite powder AM can present some porosity, it has been tested that relative density of 99.9% can be achieved with accurate laser power and scanning speed settings [46].

As it happens with casting, forging or other metal working techniques, SLM leads a particular microstructure. For some metals, it has been tested that powder bed fusion manufacturing provides a fine and homogeneous microstructure and similar elastic modulus for different printing directions. Moreover, tensile strength and ductility are higher compared with their cast versions but yield stress and ultimate tensile stress are lower for some metals. For instance, AlSi10Mg powder melted tensile strength came out to be better than cast aluminum 356 and approximate to wrought Al 6061-T6 [29].

Referred to fatigue, due to that fine grain size, strength is higher when the as-built surface is machined since rough finishing may cause crack initiation spots. Even though, results are much better for AM manufactured metals compared to cast specimens, and similar or slightly better than wrought specimens, depending on the material. Also, creep resistance notably exceeds the one presented in both wrought and cast versions, in the case of Inconel [29].

### 2.2.5. PLA properties for modeling

Polylactic acid is a biodegradable polyester obtained from vegetal resources like corn starch. It is widely used for 3D printing in medicine and industry due to its properties (see table 2.3) and its ease of use. It can be present as pure PLA or as a composite material, reinforced with additives like metals or fibers that improve one or several mechanical or physical properties [47].

**Table 2.3. PLA properties [48]**

Density	1.24 g/cm <sup>3</sup>
Ultimate Tensile Strength	45.6 MPa
Tensile Yield Strength	49.5 MPa
Modulus of Elasticity	2.3 GPa

### 2.3. Topology optimization

Thanks to the mentioned unrestricted geometry advantages, topology optimization can be applied to any part being a notable feature of AM. The aim of a topology study is to improve the structural efficiency of a single part or an entire assembly without the need to sacrifice functionality because of manufacturing limitations [1].

Stanford and Dunning [49] use a two-dimensional rib-spar web (see fig. 2.19) to perform a plane wing stress study and its respective topology optimization for several stress conditions, as it changes during the flight and before and after it happens. As a result, they get a different optimized geometry for each of the wing elements: some of them resulting as a complex shape, some stay with no mass reduction and some others are completely eliminated (see figure 2.20).

A big mass reduction comes of this study, giving a detailed structure for each element. Hence, the ideal topology study is the one taking into account every load case so the wing is able to stand them.

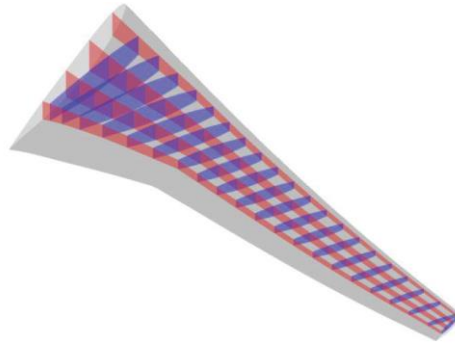


**Fig. 2.19. Wing rib-spar web [49]**

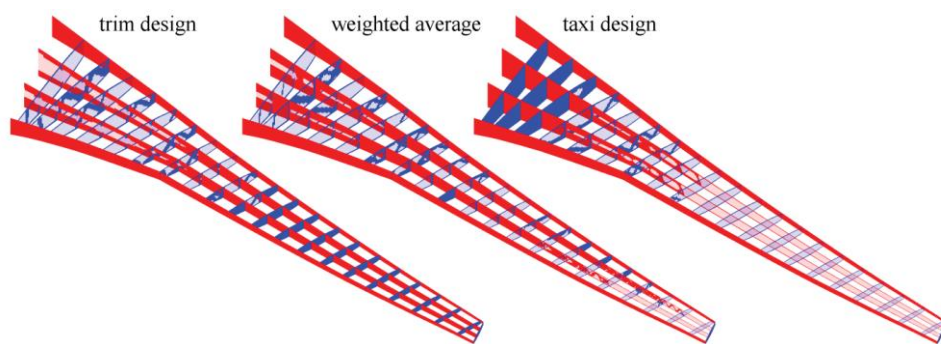


**Fig. 2.20. Topology studies results [49]**

Based on this mathematical discipline, some engineering programmers have developed algorithms for generative design tools. This technique applies iterative finite elements studies to find the best result for a given problem. Each iteration gives the best and the worst result and updates the solution as the last best result. Every sub-iteration is studied until they converge to the optimum structure [50].

Solid Edge by Siemens counts with generative design, it is able to optimize solids depending on four inputs, material properties and mass reduction and accuracy level. These mentioned four inputs are: design space, preserved regions, fixtures and load directions and magnitudes.

After that, the study is accomplished in function of the desired mass reduction which can be freely selected. Several studies can be made with the same inputs varying the percentage of mass reduced as it can be seen in fig. 2.21. The precision level, from 1 to 300, alters the number of iterations to carry out. The higher the level, the more accurate the geometry is.



Fig. 2.21. Mass reduction level effect [51]

## 2.4. Wing ribs

Wings structure can be designed for a wide variety of uses, so depending on the aircraft type wings would be thought to execute different functions. Whether they are full cantilever or not, wings need to stand certain loads produced by lift forces, the weight of all parts attached to it, such as the landing gear or the engines, and its own weight, all represented in figure 2.22. Each of them acts in a different manner depending on the dynamic movement of the airplane and external factors as wind speed and direction [3].

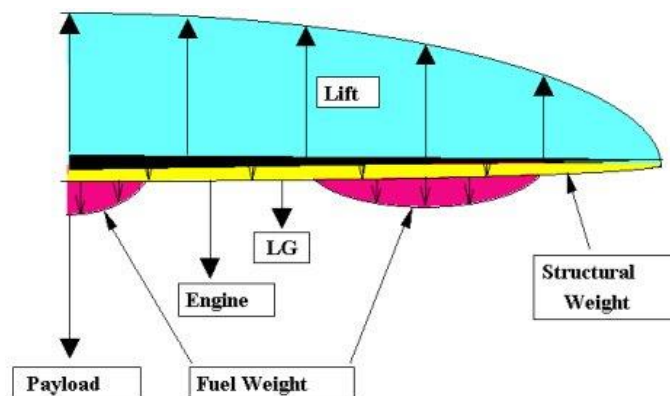


Fig. 2.22. Airplane wing loads [52]

The internal structure is formed by spars, ribs and stringers (see figure 2.23). Spars are beams to which the rest of elements are fixed, they support all distributed loads as well as punctual ones, then transmit them directly to the plane fuselage. Ribs are attached to spars, creating the cross-sectional shape and supporting loads in that direction through the entire wing. Finally, stringers and wing skin are attached to the ribs and transfer loads to them. The skin also forms the external shape and acts as a load distributor [3].

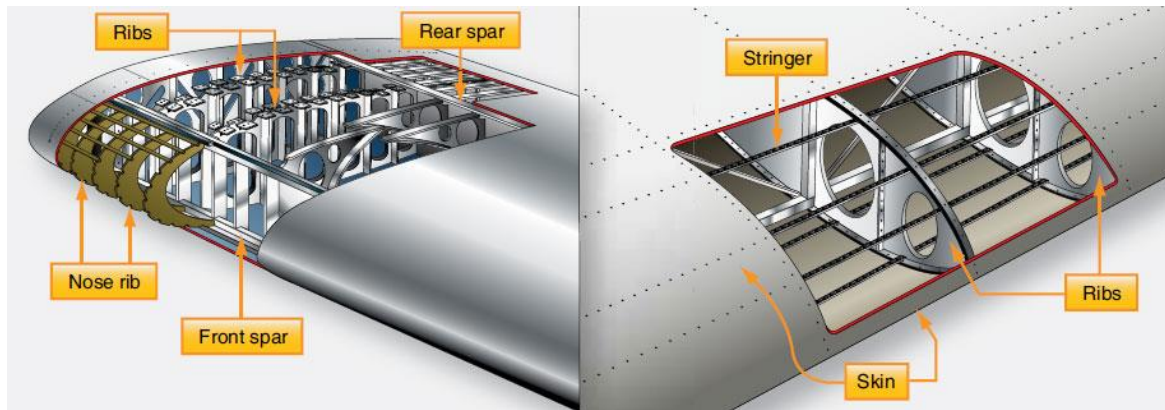


Fig. 2.23. Parts of wings structure [3].

As an approximation, figure 2.24 shows all possible loads that a wing can support represented by arrows: distributed pressures from outside air is beamed to ribs and the momentum produced both at leading and trailing edges.

Ribs gather forces and transfer them to spars, therefore, spars are considered the support device for ribs. As the actual fixing data is not known, because of its complexity, ribs can be assumed as beams simply supported and full fixed to spars.

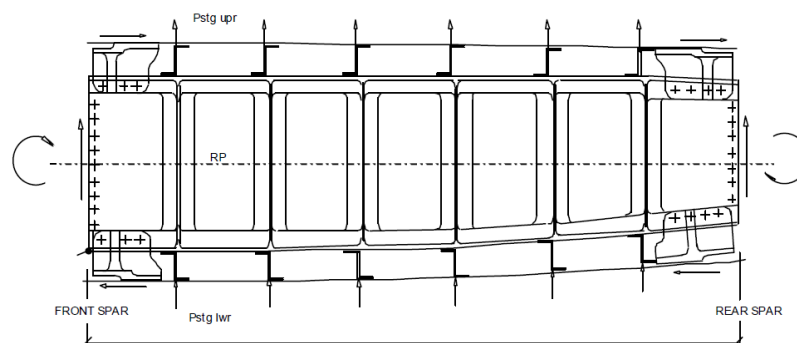
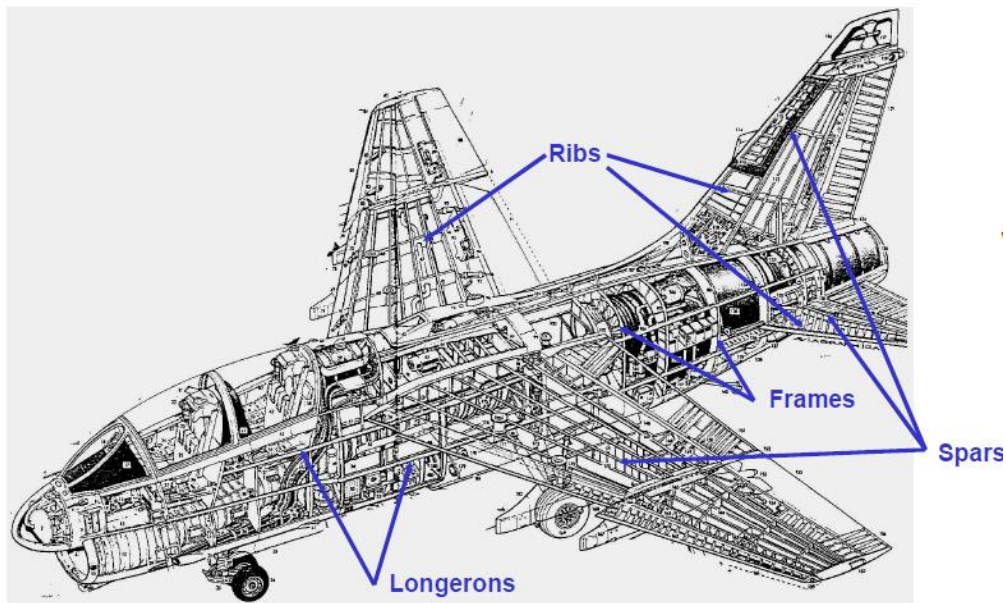


Fig. 2.24. Rib loads [53]

### 2.4.1. Types and materials

Ribs are present not only in wings but also in horizontal and vertical stabilizers (see figure 2.25) and ailerons, so there exist plenty of types and shapes for these parts. Moreover, just inside wings there can be found different types of ribs with precise functions: nose ribs, butt ribs (bulkhead or compression ribs) and main ribs.



**Fig. 2.25. Ribs at different locations [53]**

This fact makes rib design a complex task as there is a large number of different ribs inside the same aircraft and each of them must be designed individually, with specific processes and machining tools or dies, in the case of stamping.

### Materials

Materials used in wings components are determined by strength to weight performance and cost constraints. Composite materials, wood, many different metals or a combination of some of them are the suitable materials, but aluminum is the most used one [3]. For each type of part, it is chosen a material that can withstand the corresponding load and deformation being as light as possible and with the maximum fatigue resistance.

As mentioned in section 2.2.4, wings are usually made from aluminum but it appears as heat treated Al alloys as Al6061-T6, which is a suitable material for the construction of wing components.



### 3. PROBLEM APPROACH

As it has been described before in this work, AM is able to improve, optimize or even eliminate several problems of traditional manufacturing and it can follow the aim of lightening aircraft structures to improve fuel efficiency. That is the reason why aerospace industry seeks for any non-necessary weight elimination in the whole aircraft.

Thanks to finite element methods it is possible to analyze the minimum mass needed for structural elements depending on its load case, material and the space available for its placement. One of the principal elements of aircrafts are wing ribs. They support a wide variety of loads and need to be designed properly. However, not every rib needs the same mass at the same place, so mass distribution can be optimized and reduced on those places where it is not needed.

For that matter, precise data can be gathered from an existing plane during flight to know the working loads that each of its ribs supports. Using those values and applying them to a CAD model of each rib, optimum geometries can be calculated by a finite element topology study [1] and created by generative design tools. For this project the load data applied are based on the approximation described in section 2.4.

Then, the new designs are tested experimentally on 3D-printed models to find the best solution for lightening.

This chapter describes the project process, how models are designed, printed and tested. Then, a price estimation is studied to evaluate the material cost difference between machining and selective laser melting. Finally, some standards about additive manufacturing are proposed as the regulatory framework.

#### 3.1. Generative designed rib

The new ribs would be very expensive to manufacture or impossible even with most advanced machining centers. However, AM is able to create complex external and internal shapes, like hollow spaces where no mass is needed. Also, no process needs to be designed since printers are fully autonomous from CAD to the final part and riveted components can be designed directly joint as no direction restrictions exist, as it was explained in Chapter 2. These advantages permit to continuous manufacture and improve lead-time and costs of each new rib, apart from the base mass reduction improvement.

Then, the possibility of designing ribs from generative design tools like Solid Edge makes real topology optimized models for later testing.

The most suitable solution with a low budget is the printing of scaled rib models previously designed on Solid Edge for testing, described in the following chapter.

To obtain more realistic results the base taken for this work is a central rib between spars which follows a NASA SC(2)-0610 airfoil used on the Airbus A380 [54]. The coordinates of its shape are available at UIUC, accessed from Airfoil Tools and showed at Annex 1.

Using those x-y coordinates gathered in Annex 1 and importing them to Solid Edge, SC(2)-0610 airfoil is shown in figure 3.1.

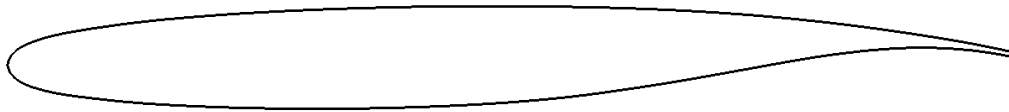


**Fig. 3.1. SC(2)-0610 airfoil**

Then, as the test is focused on a single rib, it is only considered the contour of this rib between two spars taking as a reference the wing in figure 3.2, to implement it to the previous airfoil. It appears in figure 3.3.



**Fig. 3.2. A350 wing box section [55]**



**Fig. 3.3. SC(2)-0610 airfoil with rib shape**



Finally, it is possible to sketch the shape of the desired rib and give it a certain depth. As an approximation, this depth will be a 5% of the rib total length, extruded from the sketch plane. This is translated into a 220 mm horizontal length and 12 mm depth.

Following the steps explained in Chapter 3, the volume designed on Solid Edge is given both restrictions and forces close to flight loads and then, the best geometry to support the given conditions is generated by iterative calculations, subtracting useless mass from those places where tension is lower. Giving as a result a part like the one appearing in fig. 3.4.



**Fig. 3.4. SC(2)-0610 airfoil with generative designed rib**

In the next figure (fig. 3.5) loads (arrows) and constraints (dots) have been shown, being those the best approximation possible to the rib loading theory stated in Chapter 2, but only taking into account distributed vertical loads which act as bending moment onto the rib, in that case fully fixed to the spars. It has been chosen only the bending case out of all the existing forces as the most accurate study from the possible ones available in the UC3M workshop, needing an Instron Universal Testing machine and some utillage to properly apply loads and restrictions.

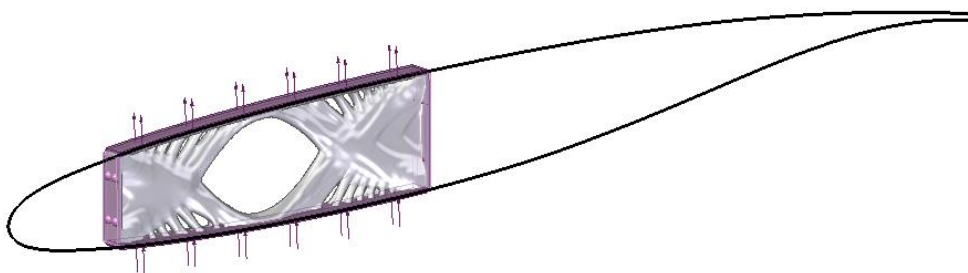


**Fig. 3.5. Generative designed rib with loads and constraints**

Generative design tool permits to vary the percentage of mass removed on the study. For a complete comparison three different mass reduction levels have been calculated: 60% (figure 3.7), 70% (figure 3.8) and 80% (figure 3.9). All of them have been printed with a square grid filling (see figure 3.10) for a more notable weight and time reduction and the 60% one both with square and triangular grid (see figure 3.11). Moreover, a rib with

vertical and horizontal stiffeners (figure 3.6) has been printed too in order to compare the other ones with a more realistic structure. This last rib is printed also with square internal grid for a more accurate comparison.

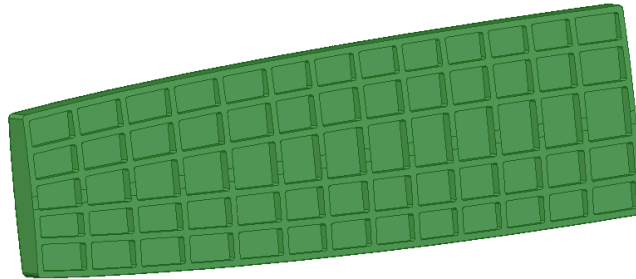


**Fig. 3.6. Rib 1.**



**Fig. 3.7. Rib 2 and 3.**

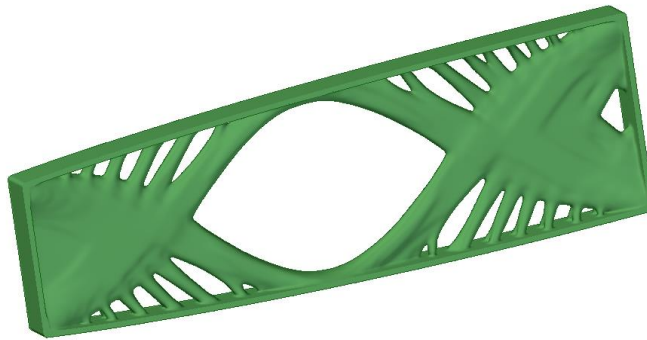


**Fig. 3.8. Rib 4.**

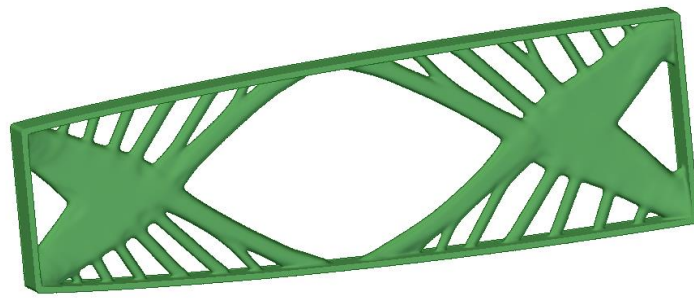


**Fig. 3.9.** Rib 5, 6, 7 and 8.

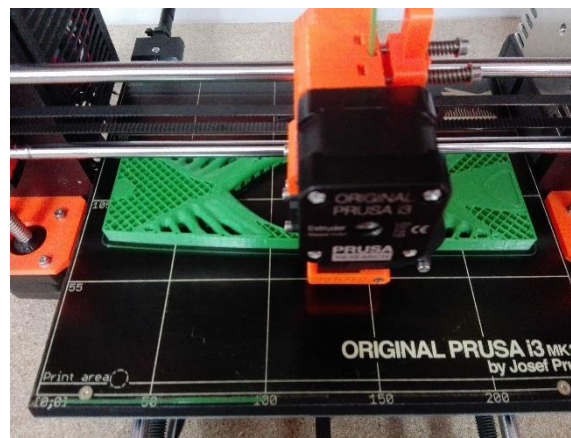


**Fig. 3.10.** Square grid filling

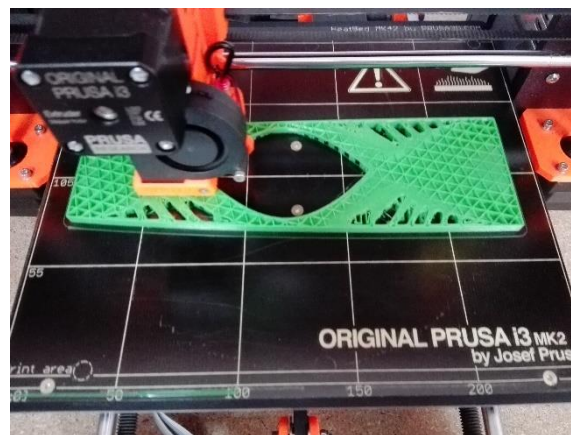


**Fig. 3.11.** Triangular grid filling

A real aluminum 3D printed rib would not be printed with the same filling pattern but with more complex ones or even full solid. This work is focused in the relative term between different structures keeping constant the rest of properties and characteristics,

except from the triangular grid rib which will try to show the influence of internal structure on additive manufacturing since it is one of the main features that can be changed and optimized and could not in traditional manufacturing.

Fig. 3.12 sums up the different parts printed and their characteristics. Each of them is labeled for a better identification. Ribs 1, 2, 3, 4 and 5 are the tested parts, ribs 6, 7 and 8 are identical to rib 5 and will be the three first trials for a proper calibration and to show the possible errors to be solved.

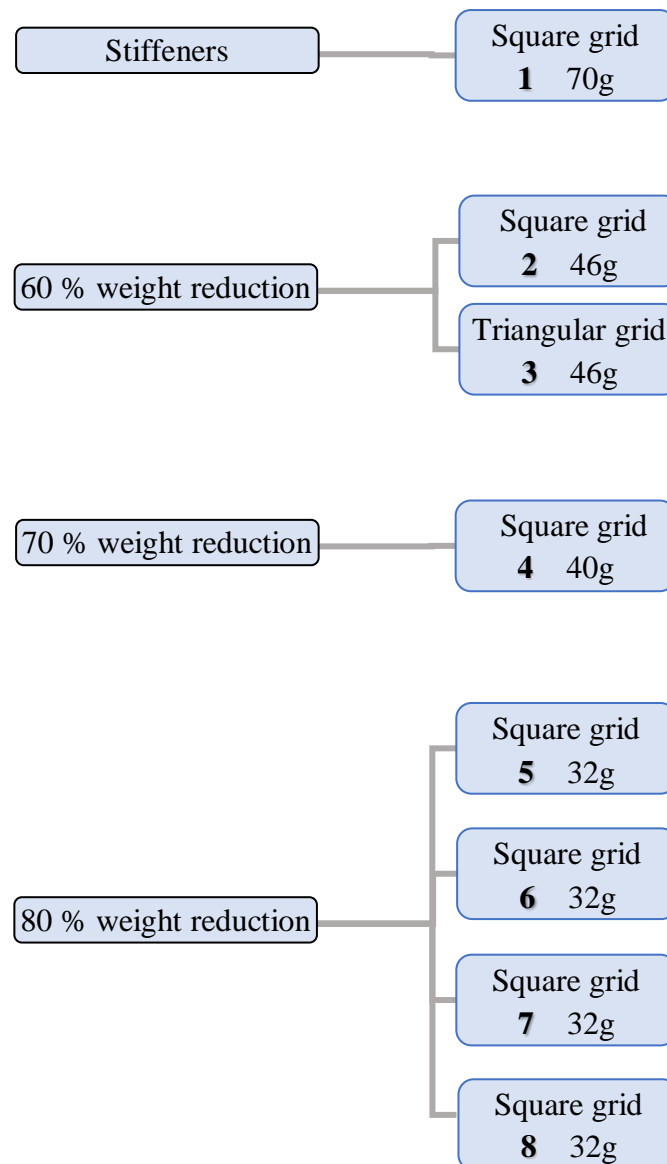


**Fig. 3.12. Ribs characteristics**

The FDM printer used for the eight ribs is a Prusa i3 Mk2S, showed in fig. 3.13, available at the Maker Space of UC3M. It presents the following characteristics [56]:

- Working volume: 10500 cm<sup>3</sup> (25 x 21 x 20 cm).
- 0.4 mm nozzle for 1.75 mm filament.
- Layer height from 0,05 mm.
- 70W average electrical consumption using PLA.
- Printable materials: PLA, ABS, PET, HIPS, Flex PP, Ninjaflex, Laywood, Laybrick, Nylon, Bamboofill, Bronzefill, ASA, T-Glase, carbon fiber compounds, Polycarbonates, etc.



**Fig. 3.13. Prusa i3 Mk2S [57]**

In addition, the material used is green BQ PLA (fig. 3.14), knowing the following properties [58]:

- Filament diameter: 1,75 mm.
- Density: 1,24 g/cm<sup>3</sup>.
- Recommended printing temperature: 200-220 °C.
- Flexion temperature under load: 56 °C (ISO 75/2B).
- Fusion temperature: 145-160 °C (ASTM D3418).
- Glass transition temperature: 56-64 °C (ASTM D3418).



**Fig. 3.14. BQ PLA filament [59]**

Once the designs are ready, it is necessary to slice them and to generate a G-code readable by the printer. This is made by Cura software, which needs an stl file to start. Then, several parameters as size and orientation must be selected. All ribs are printed in the same direction and with the same size, as showed in fig. 3.15. and 3.10.

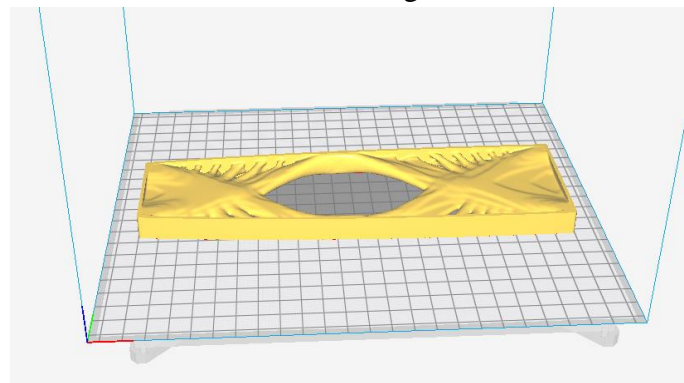


**Fig. 3.15. Printer and rib representation in Cura**

The following table, 3.1, gathers some parameters for each of the ribs: printing time and material used in mass and length. Appart, all of them share the principal manufacturing parameters for FDM: 20% inside filling, 0.15 mm layer thickness, 210 °C nozzle temperature and 60 °C hot bed temperature.

**Table 3.1. Ribs printing time and material.**

Rib	Time	Material mass	Material length
1	9h 24'	72g	24.10 m
2, 3	6h 10'	48g	16.15 m
4	5h 33'	42g	14.03 m
5, 6, 7, 8	4h 19'	33g	11.01 m
	44h 33'	276g	114.47 m



It is possible to appreciate a difference between the parts weight and the material mass needed for each of them. This is due to the material needed to print the support for those areas inclined more than  $50^\circ$ . It is printed vertically from the base to the rib surface. As it is seen in figure 3.16 (1% completed), support pattern is always a straight line stretching from side to side until touching the part body. Figure 3.17, with a 10% completed, shows how layers are printed onto the support previously printed.

The amount of lost material is about 2g for ribs 1, 2, 3 and 4 and about 1g for ribs 5, 6, 7 and 8. Support is only printed under those areas where the rib exists, therefore ribs with more blanks need less support material.

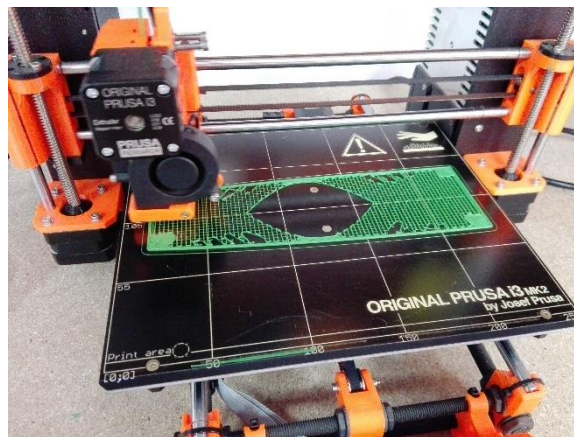


**Fig. 3.16. Printing 1 %**

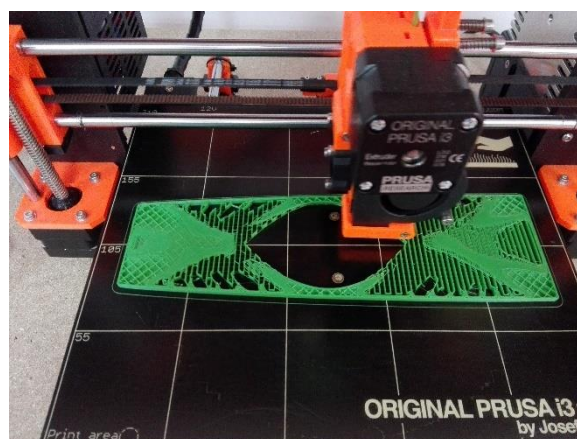


**Fig. 3.17. Printing 10%**

### 3.2. Comparison of machining and 3D printing material efficiency

To prove one of the advantages of AM it is logical to compare an AM process to a machining process. This advantage is the big savings in raw material against the material wasted in machining. The chosen part needs to be machinable and printable to make possible the fabrication in both ways. For that reason, it has been selected a part designed and manufactured by Mastercam, of which the manufacturing data is provided.

As the manufacturer does not specify the exact weight of the rib, to accurately calculate the weight and volume of material used, it has been developed a copy of the machined rib in Solid Edge (see figure 3.19), taking the dimensions from figure 3.18 and knowing the weight of the initial aluminum block. This copy has been done to calculate an estimation of the material cost if it was selective laser melted and, after that, compare it with the price of the aluminum ingot used for machining.

Mastercam's wing rib (figure 3.18) is a scaled down rib made for testing the “dynamic motion technology” and it has the following specifications [60]:

- Made of 6061-T6 Aluminum
- Total process time of 40 minutes starting after its fixture.
- Buy-to-fly ratio of 25 (raw material mass divided by final part mass): 20 lbs of Al to get an almost 2 lbs part what means about 90% of material waste.
- Whole part machined with climb milling method.

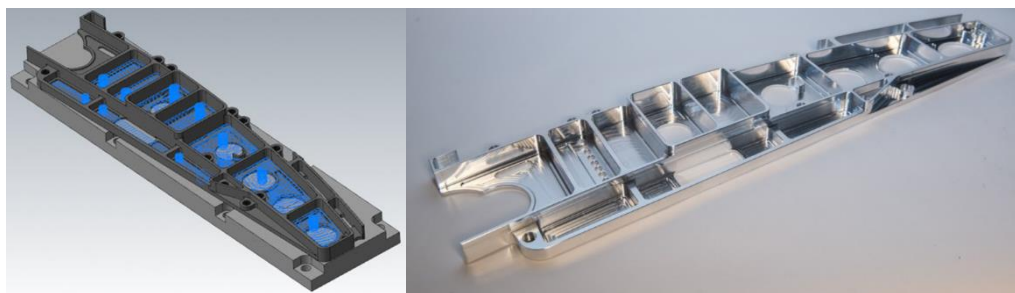
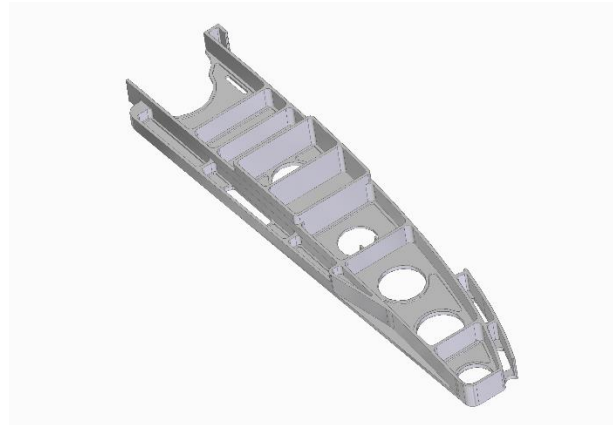


Fig. 3.18. Mastercam wing rib [60]





**Fig. 3.19. Solid Edge rib**

Once the part is done, the software provides the total mass and volume after introducing Al 6061-T6 as the part material: 1.099 kg and 405236 mm<sup>3</sup>. As explained in Chapter 2, AM parts are not full solid because of porosity. For SLM of aluminum there exists certain porosity, but with the right settings, 99.9% of density can be achieved as mentioned in the previous chapter. Thus, it is taken the same density as the machined material which is 2712 kg/m<sup>3</sup> for the calculation.

Also, buy-to-fly ratio in AM can be averaged as 1.5 [61] since support material is typically used in most methods, as the part illustrated in figure 3.20. Therefore, as the rib does not need material support it is considered buy-to-fly ratio as 1.



**Fig. 3.20. Buy-to-fly ratios [61]**

Taking into account a price of 72 €/kg [62] for Al 6061 powder, the AM part costs 79.13 € while the machined one, at a price of 2.34 €/kg [63] for a 20 lbs (9.07 kg) part, costs 21.22 €. The total price results more economical for machining but more material efficient for additive manufacturing.

It must be considered the equipment utilized, which consists of expensive machines for both cases but needs specific and wearable tooling in the case of machining. Therefore,

to the price of machined parts, it has to be added the price of inserts spent and specially designed tools depending on cutting parameters or direction.

### 3.3. Regulatory framework

Additive manufacturing is a relatively new technology and it has been introduced in industry in the last few years, therefore the standards available are limited in comparison with other methods. There exist some national and international standards which regulates the main aspects of additive manufacturing, available at AENOR:

- UNE-EN ISO/ASTM 52915:2016: Specification for additive manufacturing file format (AMF) Version 1.2. [\[64\]](#)
- UNE-EN ISO 17296-2:2015: Additive manufacturing. General principles. Part 2: Overview of processes and feedstock. [\[65\]](#)
- UNE-EN ISO 17296-3:2014: Additive manufacturing. General principles. Part 3: Main characteristics and corresponding test methods. [\[66\]](#)
- UNE-EN ISO 17296-4:2014: Additive manufacturing. General principles. Part 4: Overview of data processing. [\[67\]](#)
- UNE-EN ISO 178:2010: Plastics. Determination of flexural properties. [\[68\]](#)

The first four standards above are responsibility of the ISO/TC 261 committee of additive manufacturing and they regulate the key aspects of this technology. UNE-EN ISO/ASTM 52915 states the basis and details of a new format specialized for additive manufacturing, AMF, to substitute the traditional stereolithography format (STL). The UNE-EN ISO 17296 group describes the different categories and methods, raw materials, test methods depending on the material and fabrication method of the parts to be evaluated and the interchange of data for manufacturers and users [\[64, 65, 66, 67\]](#).

UNE-EN ISO 17296-3 specifies which standard is the most recommended for the test in question and how to perform it. For this work, the recommended standard to take into account is the UNE-EN ISO 178, suggested for plastic parts in bending test [\[66, 68\]](#).

## 4. MODELS TESTING

As it has been mentioned in the previous chapter, ribs support a wide variety of loads, being one of them a bending moment considering the two unions with spars as clamped. Due to this fact, the experimental test which better would fix the mentioned configuration is a bending test with a uniform distributed load applied on the top surface of the rib, being both sides of the rib clamped.

For that reason, to perform the experimental test in the more realistic way, three more parts need to be manufactured for constraining the rib to two degrees of freedom and to make the load applied as distributed as possible. Several options were contemplated like aluminum machining for the supporting pieces and steel machining in a CNC center for the distributed load piece, as it needs to follow the exact NACA profile. In order to make those auxiliary parts in the most cheap and fast way, they have been 3D printed.

In this section, the experimental procedure carried out after finalizing 3D printing of each geometry is explained. As it was mentioned before, all the experimental tests were performed in a universal testing machine. Two different types of machines were used due to mechanical problems. Ribs 7 and 8 were tested first in a four-points bending test configuration (figure 4.1), after these two tests, the machine broke. Due to the failure of this first machine, the rest of tests were adapted to be performed in another universal testing machine, but in this occasion with a three-point bending configuration (figure 4.2). From each test, the force-displacement curve was obtained and compared among all the configurations studied.

The tool used presses the red part on two points enough separated to distribute the load correctly through the rib, for rib 7 and 8. For the rest of ribs, the configuration is the same, but the machine contacts the red part with a single point tool (see figure 4.2). Those tests have been performed by a universal Instron testing machine at a speed of 0.2 mm/s.



**Fig. 4.1. Four-points bending configuration**

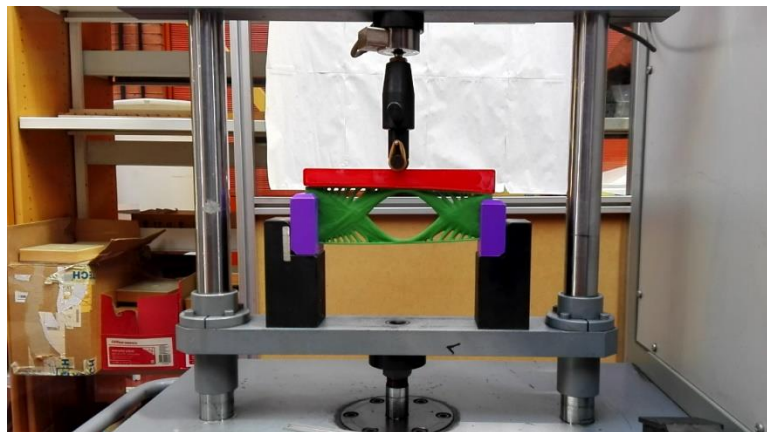


**Fig. 4.2. Three-points bending configuration**

Due to the availability of 3D printers, its simplicity of use and cost-effectiveness, the advantages of rapid prototyping and manufacturing are clearly fulfilled. As soon as the necessity of extra tooling to adapt the ribs to the press was presented, three 3D parts were developed in solid edge. After some modifications and improvements, it was possible to use those new parts in a matter of hours.

The two supports, presented in figure 4.3, are made of PLA as the ribs, but they are full solid to avoid any deformation that could affect the results. Both parts are blocks and share the same dimensions but, with the aim of keeping the rib horizontal during the test, the slot in which the rib is placed is adapted to the corresponding side of the rib. The main objective of their design is to give the ribs a larger base surface in the direction perpendicular to their plane. To reduce the total material used without investing a big time (as PLA price permits to focus in other tasks) the corners at the top are chamfered. Also,

the face where the rib stands is slightly rounded to avoid a relevant load concentration edge. The chamfering at the bottom back corner was done to adapt it to the first press metal supports and it has been also useful for the second press.

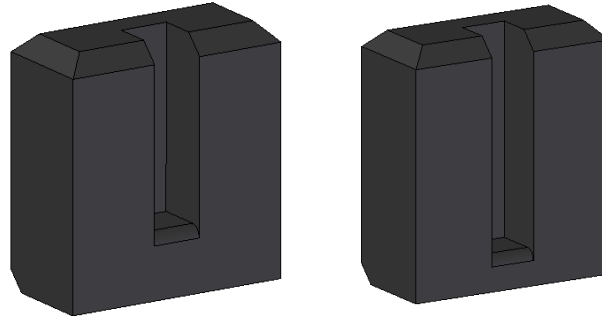


**Fig. 4.3. Support parts**

The third auxiliary part is a rectangular prism with the peculiarity that the base describes the same NACA profile as the ribs, appearing in figure 4.4. That makes that the press tool stands on the upper side of the part and it transfers and distributes the load to the whole upper side of the rib, as it does the skin on an actual rib. This one is made of ABS as PLA could be very fragile for this task and 50% filled because of ABS thermal contraction in full solid parts. Although it is partially empty inside, it does not present a significant deformation that could alter the test results. Three units of that part are built to continue with the tests in case of rupture.

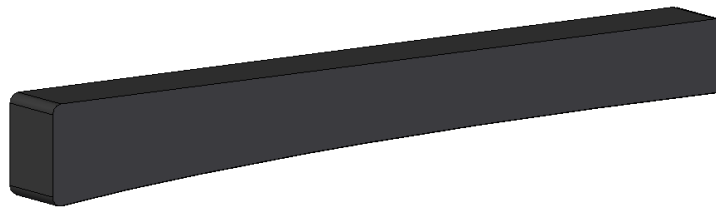


**Fig. 4.4. Load distribution part**

The full set, shown in figure 4.5 and 4.6, has been printed in different colors to make easier its visibility at the time of testing.

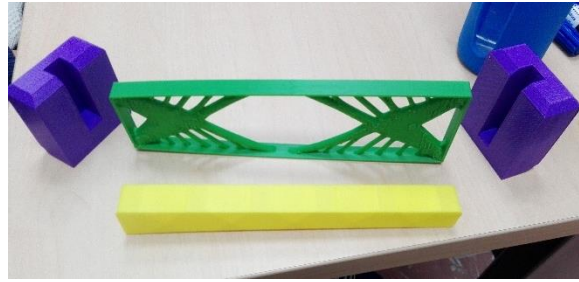


**Fig. 4.5. Model and auxiliary parts set**

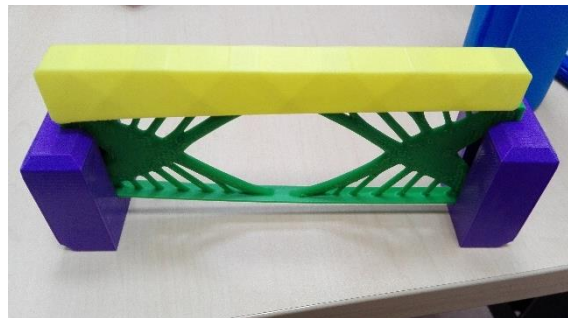


**Fig. 4.6. Mounted set**

Table 4.1 gathers the printing parameters of the auxiliary parts: time and material spent. As those parts are not optimized and they are highly infilled, the total material used is much higher than in the case of the rib models.

**Table 4.1. Auxiliary parts printing time and material**

Part	Time	Material mass	Material length
Small side support	7h 10'	121g	15.30 m
Large side support	7h 38'	129g	16.25 m
Load distributor x3	5h 6'	79g	11.27 m
	30h 6'	487g	65.36 m

The three auxiliary parts have been printed out with an Ultimaker 2 Extended+ (figure 4.7) available at the UC3M Aerospace workshop. It has the following technical characteristics [69]:

- Printing volume:  $223 \times 223 \times 305$  mm.
- 0.8 mm nozzle.
- 35W heated nozzle at 180 °C to 260 °C.
- 50 °C to 100 °C heated glass build plate.

- 600 a 20 microns layer resolution.
- Printable materials: PLA, ABS, CPE, CPE+, PC, Nylon, TPU 95A, and PP.

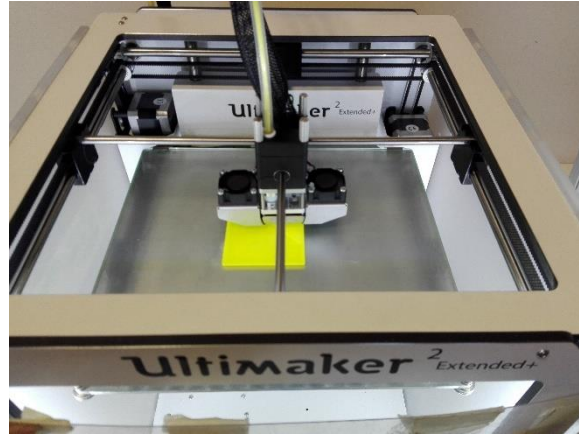


**Fig. 4.7. Ultimaker 2 extended +**



## 5. RESULTS

Once the tests are complete, the results given by the universal testing machine software are displayed in three columns: time in seconds, force in kilonewtons and displacement in millimeters. This data is easily transferred to Excel in order to represent them in graphs.

The results are analyzed for each model indicating the failure in each case, with the help of the load-displacement curves and pictures. Then, relative values are considered depending on the change of different design and printing parameters. The ribs which have been compared between each other are:

- ribs 2, 4 and 6 because of the change in the mass reduction level,
- ribs 2 and 3 because of the difference on its filling pattern,
- ribs 1, 2, 4 and 6 because of the difference between a traditional-like rib and topology optimized ribs.

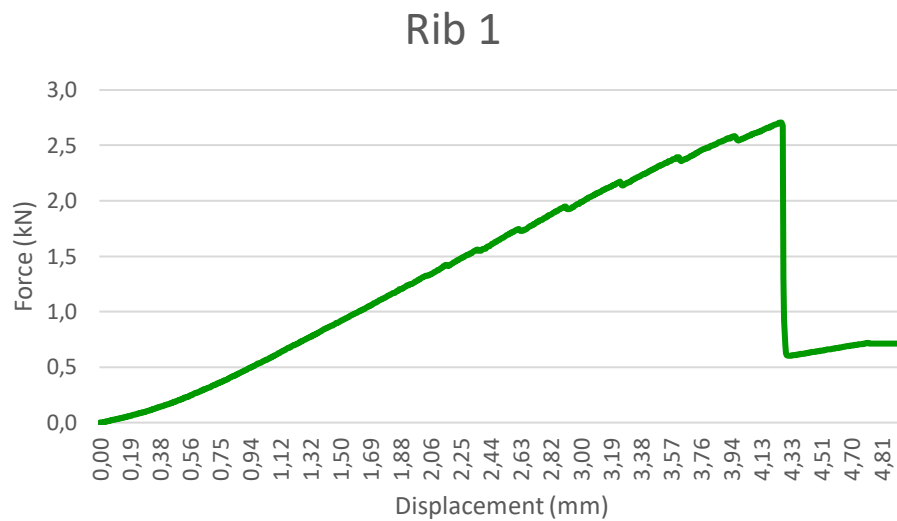
Ribs 7 and 8 are not taken into consideration as they were tested with a four-points configuration. Also, there is no picture available after the tests since the ribs broke in many pieces.

### 5.1. Individual analysis

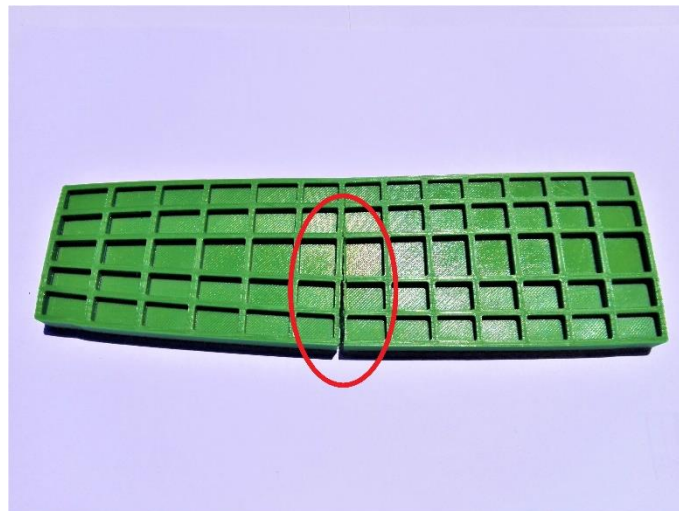
Rib 1 represents the traditional-like geometry, formed by a plane core and vertical and horizontal stiffeners. This model is taken as the reference one for later comparing and evaluate the possible benefits or drawbacks.

Figure 5.1 shows an almost straight curve until its rupture at 2.7 kN and 4.26 mm. Before the total failure, it is appreciated a series of stepped peaks caused by cracks in its internal structure. Finally, highlighted in figure 5.2, a vertical crack takes place in the middle, starting from the bottom edge.





**Fig. 5.1. Results rib1**



**Fig. 5.2. Rib 1 after the test**

In the case of rib 2, the maximum load reached before failure is 2.8 kN and the maximum vertical displacement 4.22 mm (see figure 5.3). This is the heaviest of the generative designed ribs and it has square grid filling pattern.

As rib 1, it can be seen in figure 5.3 the presence of several crack before the failure, following a linear deformation behavior, braking at the middle of the bottom fine section, circled in figure 5.4.

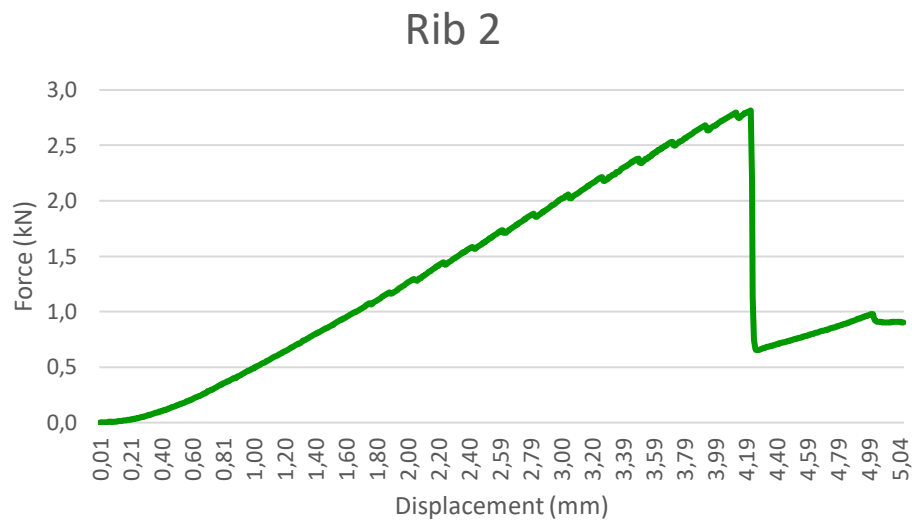


**Fig. 5.3. Results rib 2**

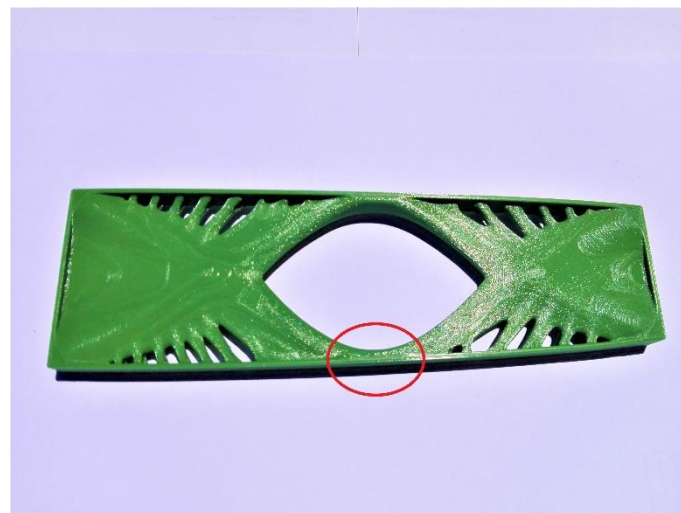


**Fig. 5.4. Rib 2 after the test**

For rib 3, the results are very similar as rib 2 because they have the same outer shape but different internal pattern, what makes a difference. The failure of the rib, seen in figure 5.5, occurs at 2.9 kN and 4.63 mm.

From figure 5.6 it is appreciated how a piece has detached from the same point of failure as rib 2. That is the most stressed spot by tension.

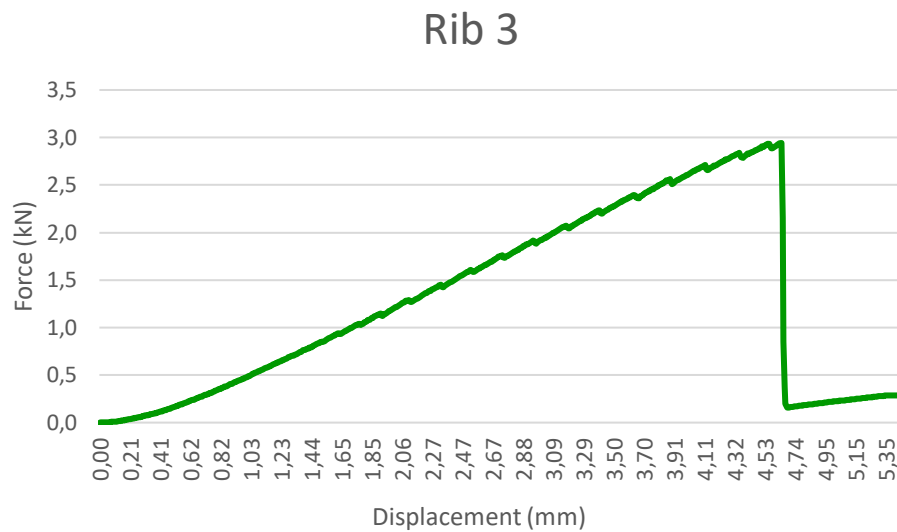


**Fig. 5.5. Results rib 3**

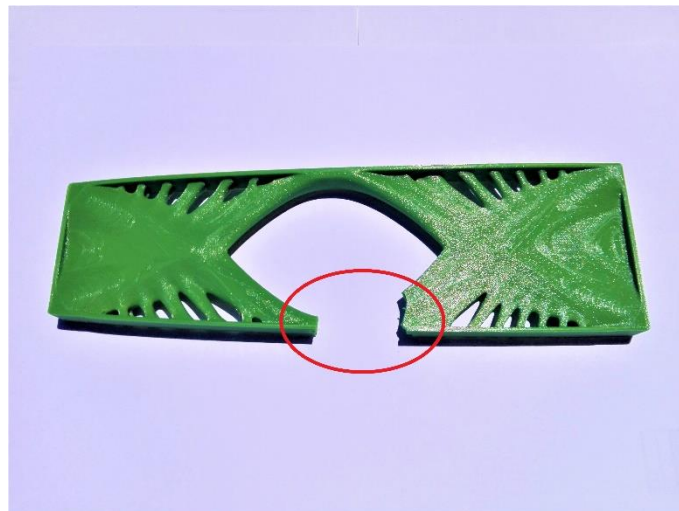


**Fig. 5.6. Rib 3 after the test**

In the case of rib 4, figure 5.7 displays a maximum load of 2.9 kN and 5.14 mm of displacement for the second heaviest model. It also brakes in stepped cracks, more pronounced as previous models.

The type of failure, marked in figure 5.8, is a clean tear at the bottom weakest section with no other deformation. This fact makes a linear deformation until braking.

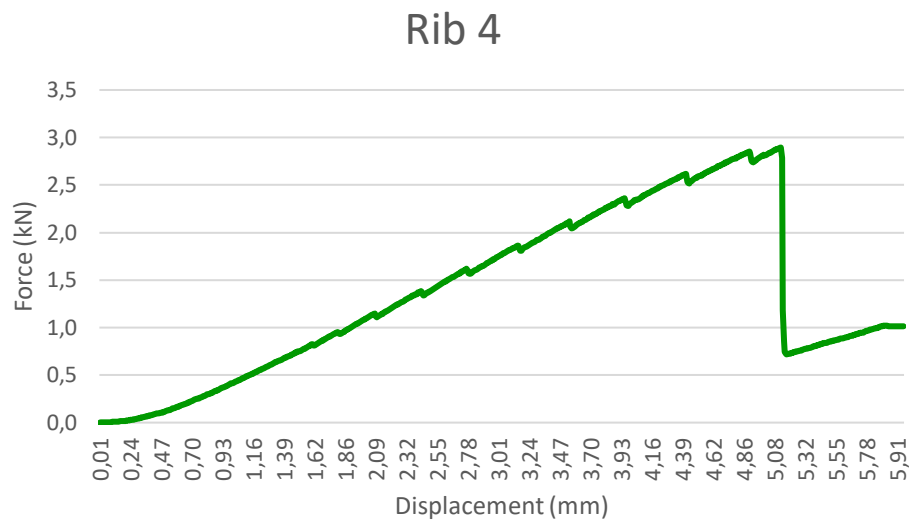


**Fig. 5.7. Results rib 4**

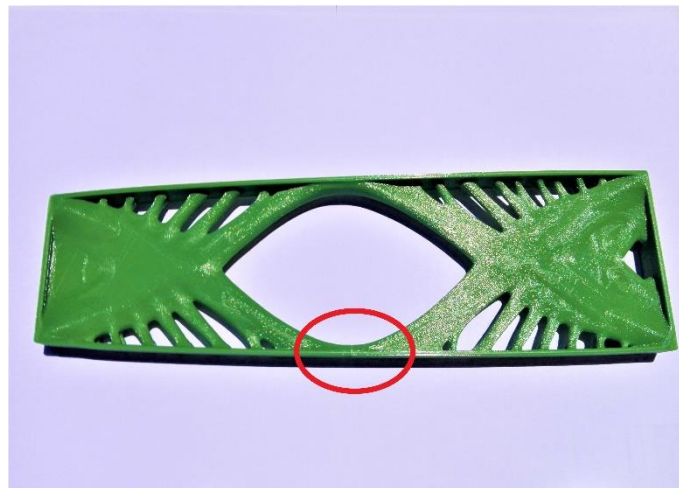


**Fig. 5.8. Rib 4 after the test**

Rib 5 is the lightest of the designs along with ribs 6, 7 and 8. This time the model breaks in three different locations (see figure 5.10), at the right-hand side edge by compression of the distribution load auxiliary part and then at the bottom side by tension.

During the test, it has been observed that this type of failure justifies the two different curvatures shown in figure 5.9. At the beginning of the test the model experiments a linear deformation until three consecutive cracks occur. After that, at a maximum load of 3 kN, the first crack takes place and the load supported slightly decreases to 2.7 kN. Finally, the second and ultimate crack occurs at 10.33 mm of displacement.

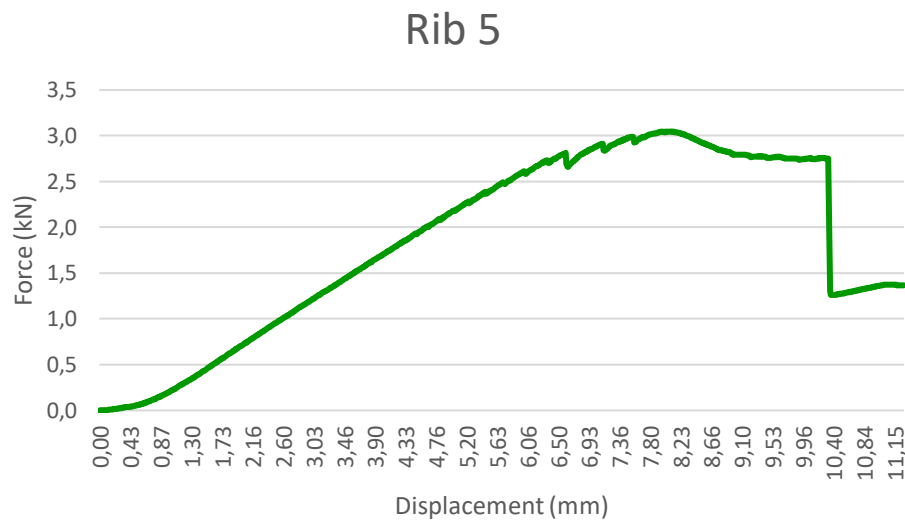


**Fig. 5.9. Results rib 5**

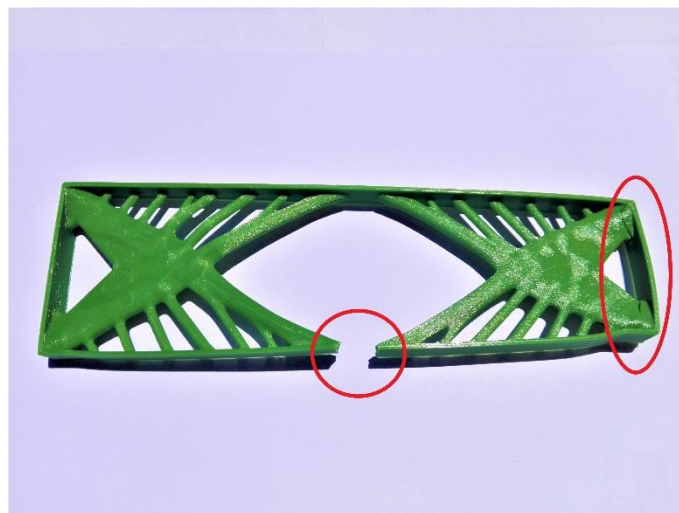


**Fig. 5.10. Rib 5 after the test**

Rib 6 shares its outer and inner characteristics as 5, but its behavior is more regular than before. The graph shown in figure 5.11 represents a linear deformation until the appearance of a large number of cracks, and the convexity upwards of the curve due to the damage at the bottom right corner by compression, highlighted in figure 5.12.

This time the ultimate failure occurs at 3.2 kN and 9 mm, better than the identical rib 5 since rib 6 has broken more homogeneously.

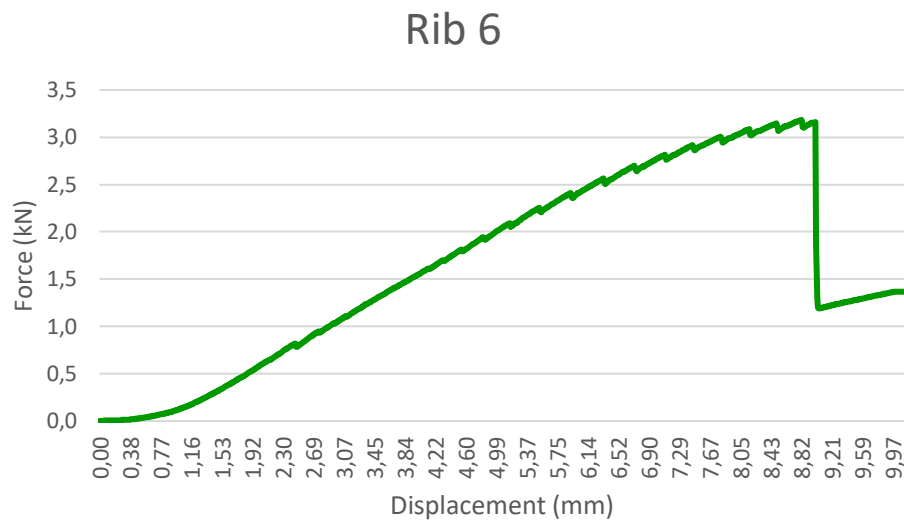


**Fig. 5.11. Results rib 6**

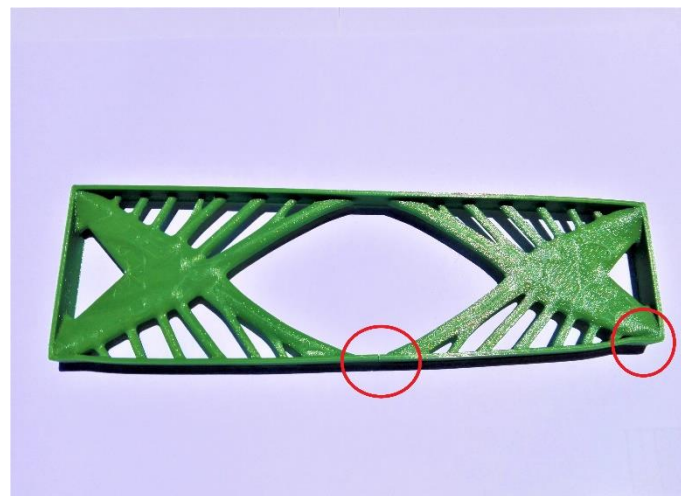


**Fig. 5.12. Rib 6 after the test**

Ribs 7 and 8 are identical to 5 and 6, and they were used as trial on the first machine and four-points bending test. Due to this fact, results were different as the described previously; they support a bending moment but also compression, as appreciated in figure 4.6.

Figures 5.13 and 5.14 display very similar patterns, the second showing a smoother and more linear function and the first affected by several small and pronounced cracks. The crack points are quite different between them: 4.1 kN and 7.94 mm for 7 and 4.9 and 14.94 for 8, very far from ribs 5 and 7. All differences may be caused due to malfunction

of the machine and, moreover, tests are different from the rest of the models, so these two results are not going to be considered in section 5.2.

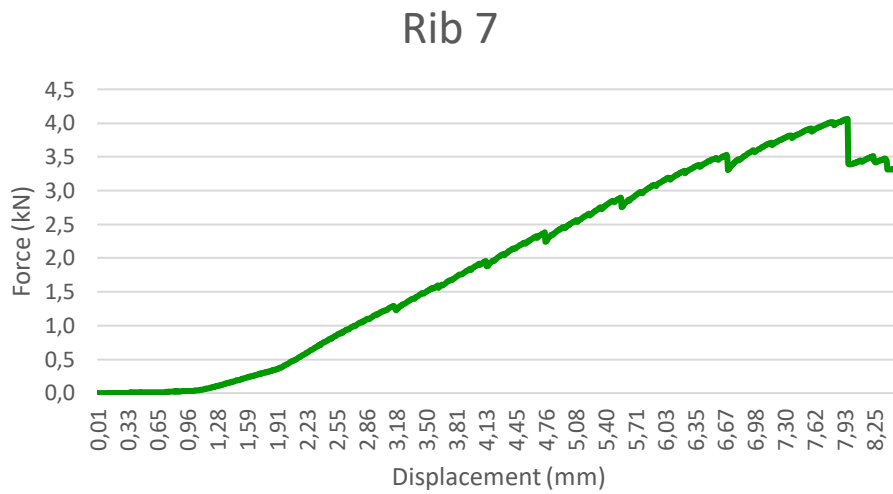


**Fig. 5.13. Results rib 7**

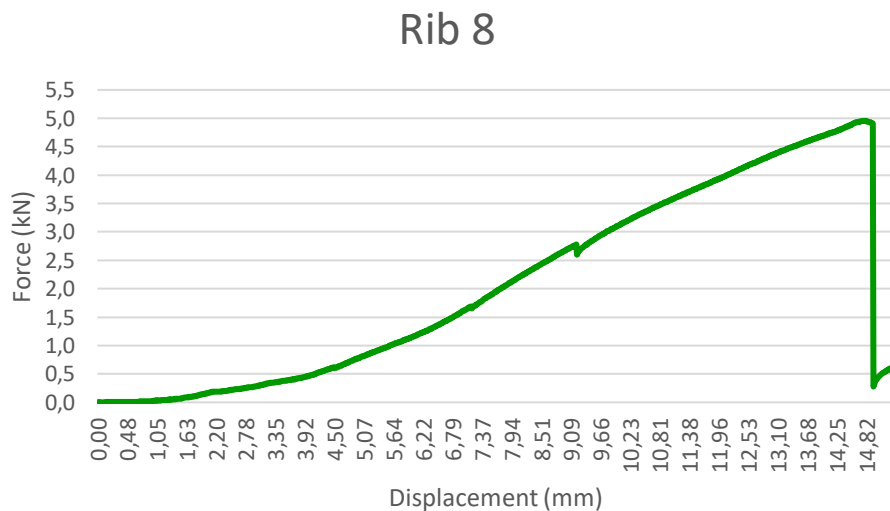


**Fig. 5.14. Results rib 8**

## 5.2. Relative results

Table 5.1 gathers the main results of each test, maximum load and maximum displacement. It is added each rib weight as well to properly compare the result according to its weight.

**Table 5.1. Tests results**

Rib	Max. load (kN)	Max. displacement (mm)	Weight (g)
1	2.7	4.26	70
2	2.8	4.22	46
3	2.9	4.63	46
4	2.9	5.14	40
5	3	8.45	32
6	3.2	9	32
7	4.1	7.94	32
8	4.9	14.94	32

There are three main changes to be considered and study separately. As mentioned before, they are mass reduction level, filling pattern and traditional shape with new generated shapes.

#### Mass reduction influence

Ribs 2, 4 and 6 share all their characteristics except the mass reduction level. Explained in Chapter 2 it is determined that for the same load case and the same generative design accuracy level, mass reduction can change from the initial volume to the minimum allowed mass before surpassing its elastic limit. The structures are set at 60, 70 and 80 % mass reduction from the initial part.

**Mass reduction level comparison**

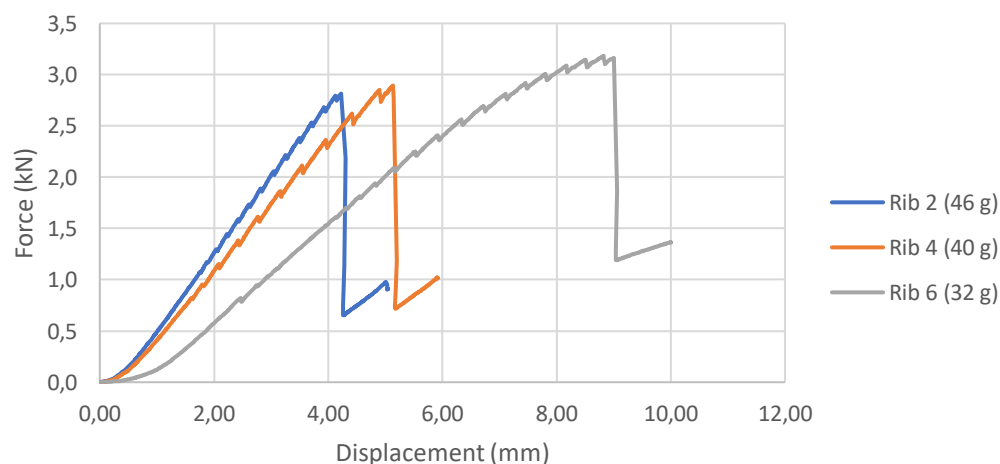


**Fig. 5.15. Mass reduction level comparison**



The differences shown by each of these models are observed in figure 5.15. It is clear that rib 2, the heaviest (46 g), is the most robust and fragile as it breaks under lower force than the others and stretches at a maximum of 4.22 mm, 0.92 mm less than rib 4 and 4.78 mm less than rib 6.

The next rib, number 4, weights 40 g and supports 0.1 kN more than rib 2, stretching until 5.14 mm. The gap between ribs 2 and 4 is 6 grams but performance is quite similar, being rib 4 for more ductile.

The most notable difference is marked by rib 6 which is the lightest one with 32 g of weight. The slope of its deformation is the lowest of the three since its shape permitted to reach a larger displacement with a similar breaking load, 3.2 kN.

This comparison shows an inverse tendency, as mass is reduced, the rib reaches higher maximum force and displacement values. However, rigidity gets affected, being heavier structures more robust and presenting a linear deformation function.

### Filling pattern influence

Ultimaker Cura software, as other 3D slicing softwares, offers a list of different filling patterns like grids or functions constant and non-constant in the Z-axis. For this project, all the models have been printed with a square grid pattern except from one printed with triangular grid pattern. Those are ribs 2 and 3 presenting square and triangular grids, respectively, being the rest of features identical.

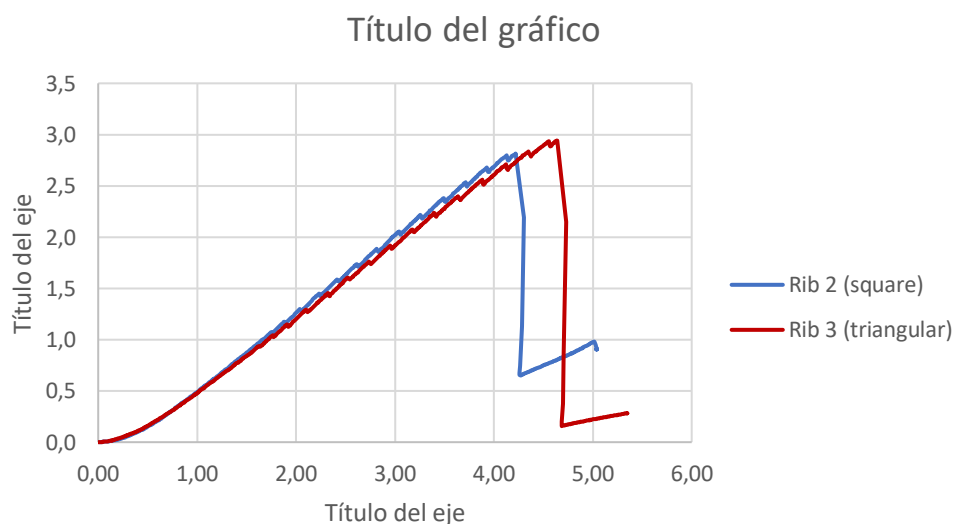


**Fig. 5.16. Filling pattern comparison**

Results of both tests are shown in figure 5.16. Both curves are almost coincident, including slope and those stepped small cracks mentioned in section 5.1. There is no significant difference until their point of failure, where rib 3 (triangular) supports 0.1 kN more and stretches extra 0.41 mm than rib 2 (square).

### Traditional and generative designed structures

The last comparison involves those ribs specially designed for additive manufacturing (ribs 2, 4 and 6) and one based on traditional manufacturing (rib 1). Figure 5.17 adds the results of rib 1 test to the graph shown in figure 5.15.

Even though rib 1 weights 70 g, against 46, 40 and 32 g of the other ribs, it supports the lowest maximum load, 2.7 kN, and reaches 0.04 mm more than rib 2. Moreover, its deformation curve is very similar to rib 2, presenting a slightly lower slope.

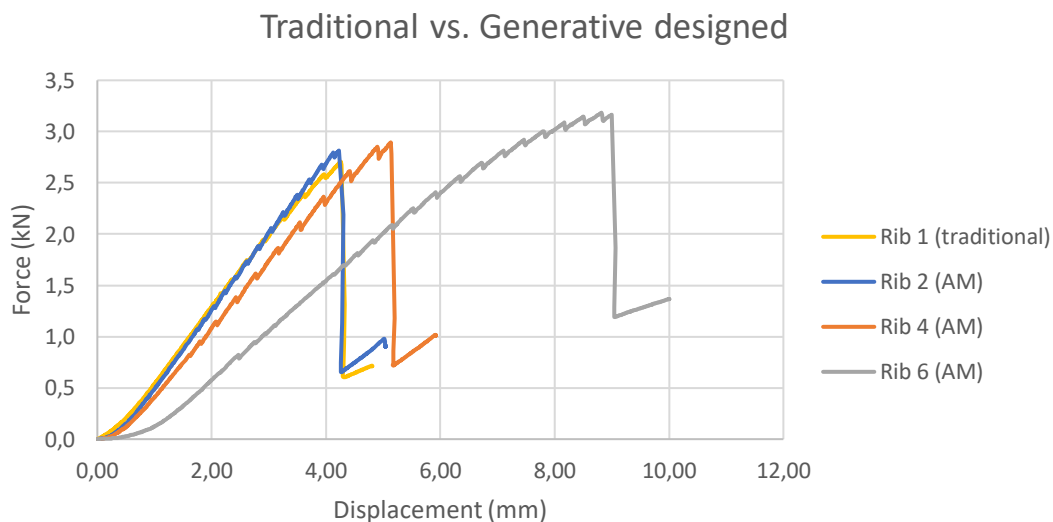


**Fig. 5.17. Traditional vs. Generative designed**

The greatest difference appears between rib 1 and 6, the heaviest and the lightest of them. It is appreciated that the extra weight of rib 1 does not make a significant difference with the following rib in weight so the comparison with the other two remains intact as the one stated at the beginning of the present section.

## 6. SOCIOECONOMIC ENVIRONMENT

### 6.1. Budget

For the fulfillment of this project, several hardware and software must be considered in addition to its energy consumption, the printing material used and the working hours spent on development, research and writing.

The following tables list the different expenses by categories. Table 6.1 enumerates the hardware equipment needed and the approximate price of them: a personal laptop [70] for web research and project writing, a laptop provided by the department in charge with Solid Edge software installed to create and calculate the 3D parts, two 3D printers [56, 69] to print the eight ribs and the auxiliary testing parts, an SD card [71] to transfer the files from the computer to the printers, pliers [72] to remove the support material from the printed pieces and the personal protection equipment (PPE) [72] required by the UC3M Maker Space.

The entire price of each has been considered as it is necessary to buy or obtain each of them to carry out the project, although they can be still used when the work is done.

**Table 6.1. Hardware budget**

Hardware	Price (€)
Laptop Asus	690
Laptop UC3M	800
Prusa Mk2S	999
Ultimaker 2 extended +	2495
SD card	15
Pliers	22
PPE MKS	25
	5036

Specialized software has been used too. Three programs, shown in Table 6.2, which are Ultimaker Cura, provided by Ultimaker completely free, Solid Edge, priced from the information of a monthly license [73] and Word and Excel included in the Microsoft Office 365 package [74].

**Table 6.2. Software budget**

Software	Unit Price	Total (€)
Ultimaker Cura	0	0
Solid Edge	402 €/month	402
Microsoft Office	100 €/year	100
		502

As this project counts with tangible experiments, a part of the budget is set aside for materials, PLA and ABS. The first is used on the ribs (276g) and the two supports (250g) and the second for the three load distributing pieces, summed up in Table 6.3.

**Table 6.3. Material budget**

Material	Unit Price	Quantity	Total (€)
PLA	17.9 €/kg	526g	9.41
ABS	20 €/kg	237g	4.74
			14.15

As well as the materials used, there is another consumable good, energy. All the equipment needed in the project have been thought to be low-power systems so the total energy used represents the lowest expense of the project. At the time of use, the approximate price of energy in Spain was 12 €/kWh [75], resulting the total price of energy calculated in Table 6.4.

**Table 6.4. Energy budget**

Device	Power (W)	Time (h)	Energy (kWh)	Price (€)
Laptop Asus	65	300	19.5	2.34
Laptop UC3M	65	40	2.6	0.31
Prusa Mk2S	70	44.55	3.12	0.37
Ultimaker 2 extended +	221	30.1	6.65	0.8
				3.82

Finally, the time contribution from an engineer taking into account the time spent for the parts design, supervision of 3D printing, evaluation and testing of the printed parts and writing of the report over five months. Considering the average salary of a mechanical engineer in Spain as 13 €/h [76], the total expense is listed in Table 6.5.

Table 6.5. Salary budget

Concept	Time (h)	Price (€)
Writing and researching	300	3900
Printing supervision	75	975
Tests	2	26
Designs and settings	40	520
	417	5421

Summing up, the total price of each of the five categories evaluated, the total budget of this project comes to 10976.97 €.

## 6.2. Socioeconomic impact

Aerospace industry, as it has been explained in this project, seeks for the maximum efficiency investing big amounts of money. To reduce fuel consumption is necessary to improve the engines performance or to decrease the overall weight.

The study carried out contributes to a significant weight reduction of the airplanes' wings structure. As weight is reduced, less energy is needed to fight against inertia during the take off and to lift the aircraft to thousands of feet.

This is translated into an important fuel saving and hence money savings. In addition, lower fuel mass would need to be transported onto the plane or larger range travels can be possible with the same fuel as conventionally.

The savings mentioned are a potential advantage for airline companies, which can benefit themselves with higher profits and their customers with cheaper flying tickets. Thus, air traveling would compete as a cheaper option than before.

As this technology is already being exploited with smaller and less important parts in aerospace, this work introduces a more ambitious application which is the remodeling of some of the principal parts of a wing. If investment keeps existing in 3D printing, it would be possible to see such an important change in real planes which step by step are built with more 3D printed parts.

Finally, environmental impact, as one of the most important problems today, requires more strict restrictions every year. Then, solutions for that danger follows the same line as higher efficiency. Also, lighter structures could make in some manner a weight margin to introduce other propulsion systems like electric motors.

Additive manufacturing in aerospace, therefore, could represent a revolution in the near future with a notable social and economic impact enhancing the investment in this industry, making large-distance traveling more affordable for a wider public and getting closer to the zero-emissions traveling.

## 7. CONCLUSIONS AND FUTURE WORK LINES

This work proposes an alternative manufacturing method for airplanes wing ribs to make this means of transport cheaper and more environmentally friendly. To achieve that goal, it is necessary to design lighter structures to save useless mass.

Additive manufacturing can produce any type of topology optimized structures, impossible to fabricate with conventional manufacturing methods. It has been analyzed the viability of generative designed structures considering their mechanical behavior in comparison with a traditional-like machined rib and evaluated the material price difference between 3D printing powder and traditional aluminum ingots.

Some conclusion came out from this study, regarding that the tests performed are not a complete reproduction of real flight loads since they only consider the bending case.

Considering the objective of evaluating the performance change when design and printing parameters are modified and the realization of experimental tests, it has been concluded:

- Generative designed rib models present higher maximum load and displacement as mass removal level increases, being rib 6 (32 g) the most resistant and rib 2 (46 g) the weaker.
- Also, 32 g rib is the less rigid and 46 g rib is the most, presenting a decreasing slope as the models are lighter.
- Filling pattern does affect strength properties. As other engineering structures, triangular web have performed better than square grid keeping the same mass and outer shape.
- Rib 1 (70 g), based on a traditional machined rib, behaves in a similar way than rib 2 (46 g), being useless the extra weight of rib 1 for this type of test.

The conclusion from the verification of additive manufacturing utility:

- Rapid prototyping has been crucial for the development of several parts of this work. First, the possibility of obtaining real models of the CAD designs, which were printed in a very short time, and second the benefit of printing specific auxiliary tooling for the experimental tests. In both cases, AM provided a cost-efficient, fast and local solution.
- Selective laser melting results a more expensive method due to the price of metal powders in comparison with metal ingots for machining, even considering the non-wasted material by AM. However, this margin can be shortened thanks to the savings in wearable tooling and the reduced weight of equivalent parts.

Those conclusions support the attainment each of the secondary objectives of this project and the main objective: to demonstrate if it is possible the substitution of regular wing ribs by generative designed 3D printed parts.

#### Future work lines

For a further development of this study, some proposals are listed below to improve and complete this work in accordance with the objectives mentioned at the beginning about making air transportation as efficient as possible.

- Implementation of composite materials as ceramics, reinforced fibers or new metal alloys in the form of printable filaments or powders.
- Use of metal-ceramic composites as a solution of porosity in additive manufactured metals [27].
- Design of an advanced measuring system to accurately gather load information of every rib of an existing airplane for a proper optimization. Counting with this information, generative design analysis can provide a tailored part able to support exactly the forces that it needs, resulting a mass fully exploited.
- Explore other structural parts suitable to be optimized and 3D printed for the sake of a general lightening. Any aircrafts if formed by thousands of parts, so it is possible to reduce the total weight significantly.
- Further research in fatigue and crack propagation in printed metals. Those are common problems in aero structures and there is certain lack of information about theses phenomena in additive manufacturing in comparison with traditionally produced metals.
- Testing the possibility of full solid parts or alternative filling patterns. SLM (as other methods) can print a large number of filling patterns with different infill percentage. It would be important to find the optimum pattern to reduce weight as much as possible.



## 8. REFERENCES

- [1] L. Krog, A. Tucker and G. Rollema. "Application of Topology, Sizing and Shape Optimization Methods to Optimal Design of Aircraft Components". Altair. <https://www.altair.com/resource/detail/687> (access: 9/2/2019).
- [2] P. H. Moreira Magalhães. "New materials being used in aircraft industry". Aero Coatings. <https://degradationworld.wordpress.com/2014/12/14/new-materials-being-used-in-aircraft-industry/> (access: 6/6/2019).
- [3] "Wings". Flight mechanics. <http://www.flight-mechanic.com/> (access: 1/3/2019).
- [4] R. Liu, Z. Wang, T. Sparks, F. Liou, J. Newkirk. *Laser Additive Manufacturing*. Missouri: Woodhead Publishing, 2017. [On line]. Available: <https://doi.org/10.1016/B978-0-08-100433-3.00013-0>
- [5] "SmarTech Publishing Issues 2019 Additive Manufacturing Market Outlook". Smart tech analysis. <https://www.smartechanalysis.com/news/smartech-publishing-issues-2019-additive-manufacturing-market-outlook/> (access: 6/6/2019).
- [6] Faculty of Aerospace Engineering "Aircraft & spacecraft wing structures". Delft University of Technology. [https://ocw.tudelft.nl/wp-content/uploads/AE1102\\_Structures\\_Slides\\_4.pdf](https://ocw.tudelft.nl/wp-content/uploads/AE1102_Structures_Slides_4.pdf) (access: 22/2/2019).
- [7] "Types of machining". Thomas. <https://www.thomasnet.com/articles/custom-manufacturing-fabricating/types-machining> (access: 18/5/2019).
- [8] K.S. Prakash, T. Nancharaih, V.V.S. Rao, "Additive Manufacturing Techniques in Manufacturing - An Overview", *Materials Today: Proceedings*, volume 5, issue 2, part 1, pp. 3873-3882, 2018. [On line]. Available at: <https://doi.org/10.1016/j.matpr.2017.11.642>. Access: 1/2/2019.
- [9] D. Korn. "Complete Machining of Large Aerospace Parts". Modern Machine Shop. <https://www.mmsonline.com/articles/complete-machining-of-large-aerospace-parts> (access: 18/5/2019).
- [10] R. R. Patel, A. Ranjan. "Advanced Techniques in Machining of Aerospace Superalloys: A Review". *International Journal of Advance Research in Engineering, Science & Technology*, Vol. 2, Issue 5, May 2015. [On line]. Available: <https://pdfs.semanticscholar.org/dfef/eac9e191f38b48fd1d59bea28781f64335f0.pdf>
- [11] "Structural parts; wingrib, spar, stringer". Unising. <https://www.unisign.com/applications/aerospace/structural-parts-fuselage-empirage-bulkhead/> (access: 18/5/2019).
- [12] "What is metal stamping?". Engineering Specialties Inc. <https://www.esict.com/what-is-metal-stamping/> (access: 18/5/2019).

- [13] “Forming Wing Ribs”. TM Technologies.  
<https://www.tinmantech.com/education/articles/forming-wing-ribs.php>  
(access: 18/5/2019).
  
- [14] Emily. “When to Stamp Metal and When to Fabricate – Selecting the optimum method for production”. Swift Metal Services.  
<http://www.swiftmetal.com.au/latest-news/when-to-stamp-metal-and-when-to-fabricate/>  
(access: 18/5/2019).
  
- [15] “Jason Beaver's RV-7”. Jason Beaver. <http://jasonbeaver.com/rv7/2009/04/>  
(access: 18/5/2019).
  
- [16] T. Altan, G. Ngaile, G. Shen, *Cold and Hot Forging Fundamentals and Applications*. USA: ASM International, 2005. [On line]. Available:  
<http://160592857366.free.fr/joe/ebooks/Mechanical%20Engineering%20Books%20Collection/PRODUCTION%20TECHNOLOGY/Cold%20and%20Hot%20Forging%20-%20Fundamentals%20and%20Applications.pdf>
  
- [17] P. Garre, G. Venkata Arjun, “Modeling and Analysis of a RIBS and Spars of An Airplane Wing for Bending and Shear Loads”. *International Journal for Research in Applied Science & Engineering Technology*, Vol. 5, issue 2, February 2017. [On line]. Available: <https://www.ijraset.com/files/serve.php?FID=6245>
  
- [18] M. Moure Cuadrado, “Análisis de la evolución del daño en laminados con agujero empleando la mecánica del daño discreto”, Tesis doctoral, Mecánica de medios continuos y teoría de estructuras, Universidad Carlos III de Madrid, Leganés, España, 2016. [On line]. Available: <https://e-archivo.uc3m.es/handle/10016/23456>
  
- [19] Steve. “14-07 Wing Ribs Riveted to Spar”. Van’s RV14 Project.  
<http://vansrv14project.uk/2018/08/08/14-07-wing-ribs-riveted-to-spar/>  
(access: 5/5/2019).
  
- [20] P.M. Mohite. “AIRCRAFT BASIC CONSTRUCTION”. [On line]. Available:  
[http://home.iitk.ac.in/~mohite/Basic\\_construction.pdf](http://home.iitk.ac.in/~mohite/Basic_construction.pdf)
  
- [21] “Advantages and disadvantages of welding”. Mechanical Engineering  
<http://mechanicalinventions.blogspot.com/2015/06/advantages-and-disadvantages-of-welding.html> (access: 22/5/2019).
  
- [22] “Welded tube frames”. Paolo Severin.  
<http://www.paoloseverin.it/techno/Welded/page13.html> (access: 18/5/2019).
  
- [23] B. Redwood. “Additive Manufacturing Technologies: An Overview”. 3D HUBS.  
<https://www.3dhubs.com/knowledge-base/additive-manufacturing-technologies-overview> (access: 3/2/2019).

- [24] T.D. Ngo, A. Kashania, G. Imbalzano, K.T.Q. Nguyen, D. Huib, “Additive manufacturing (3D printing): A review of materials, methods, applications and challenges”, *Composites Part B: Engineering*, vol. 143, pp. 172-196, June 2018. [On line]. Available at: <https://doi.org/10.1016/j.compositesb.2018.02.012>. Access: 1/2/2019.
- [25] P. Cain. “The impact of layer height on a 3D print”. 3D HUBS. <https://www.3dhubs.com/knowledge-base/impact-layer-height-3d-print> (access: 3/2/2019).
- [26] “Modelado por deposición fundida (FDM)”. Materialise. <https://www.materialise.com/es/manufacturing/tecnologia-de-impresion-3d/modelado-por-deposicion-fundida> (access: 7/6/2019).
- [27] A. L. Maximenko, E. A. Olevsky, “Pore filling during selective laser melting - assisted additive manufacturing of composites”, *Scripta Materialia*, vol. 149, pp. 75-78, May 2018. [On line]. Available at: <https://doi.org/10.1016/j.scriptamat.2018.02.015>. Access: 4/2/2019.
- [28] J. Zhang, B. Song, Q. Wei, D. Bourell, Y. Shi, “A review of selective laser melting of aluminum alloys: Processing, microstructure, property and developing trends”, *Journal of Materials Science & Technology*, vol. 35, issue 2, pp. 270-284, February 2019. [On line]. Available at: <https://doi.org/10.1016/j.jmst.2018.09.004>. Access: 4/2/2019.
- [29] L. Yang et al., *Additive Manufacturing of Metals: The Technology, Materials, Design and Production*. Springer International Publishing AG 2017.
- [30] C. Körner, “Additive manufacturing of metallic components by selective electron beam melting — a review”, *International Materials Reviews*, vol. 61, issue 5, pp. 361-377, May 2016. [On line]. Available at: <https://www.tandfonline.com/doi/full/10.1080/09506608.2016.1176289>. Access: 6/2/2019.
- [31] M. Galati, L. Iuliano. “A literature review of powder-based electron beam melting focusing on numerical simulations”, *Additive manufacturing*, vol. 19, pages 1-20, January 2018. [On line]. Available at: <https://www.sciencedirect.com/science/article/pii/S2214860417300635>. Access: 7/6/2019.
- [32] F.P.W. Melchels, J. Feijen, D.W. Grijpma, “A review on stereolithography and its applications in biomedical engineering”, *Biomaterials*, vol. 31, issue 24, pp. 6121-6130, August 2010. [On line]. Available at: <https://doi.org/10.1016/j.biomaterials.2010.04.050>. Access: 6/2/2019.

- [33] Franky. “3D Printing Technologies: Stereolithography”. MAterialise. <https://i.materialise.com/blog/en/an-intro-to-our-3d-printing-technologies-stereolithography/> (access: 7/6/2019).
- [34] H. N. Chia, B. M. Wu. “Three-Dimensional Printing of Tissue Engineering Scaffolds”. Sigma-Aldrich. <https://www.sigmaaldrich.com/technical-documents/articles/materials-science/three-dimensional-printing.html> (access: 7/6/2019).
- [35] Y. S. Liao, H. C. Li, and Y. Y. Chiu, “Study of laminated object manufacturing with separately applied heating and pressing”, *International Journal of Advanced Manufacturing Technology*, vol. 27, issue 7-8, pp. 703–707, January 2006. [On line]. Available at: <https://link.springer.com/article/10.1007/s00170-004-2201-9>. Access: 5/2/2019.
- [36] “Laminated Object Manufacturing”. Efunda. [https://www.efunda.com/processes/rapid\\_prototyping/lom.cfm](https://www.efunda.com/processes/rapid_prototyping/lom.cfm) (access: 7/6/2019).
- [37] “Modeling technology platform”. Siemens. <https://www.plm.automation.siemens.com/global/en/products/mechanical-design/modeling-technology-platform.html> (access: 19/3/2019).
- [38] S. Hendrixson. “3 Ways Volkswagen Will Use HP Metal Jet”. Additive Manufacturing. <https://www.additivemanufacturing.media/blog/post/3-ways-volkswagen-will-use-hp-metal-jet> (access: 3/3/2019).
- [39] R. Dvorak. “Czech Republic: The role of 3D printing technology in the innovation process”. MM Industrial. <https://www.maschinenmarkt.international/czech-republic-the-role-of-3d-printing-technology-in-the-innovation-process-a-616126/> (access: 3/3/2019).
- [40] C. de Vries. “Volkswagen Autoeuropa: Maximizing production efficiency with 3D printed tools, jigs, and fixtures”. Ultimaker. <https://ultimaker.com/en/stories/43969-volkswagen-autoeuropa-maximizing-production-efficiency-with-3d-printed-tools-jigs-and-fixtures> (access: 3/3/2019).
- [41] A. Derver. “Airbus Prints Titanium Part For A350 Pylon”. MRO-Network. <https://www.mro-network.com/manufacturing-distribution/airbus-prints-titanium-part-a350-ylon> (access: 8/4/2019).
- [42] “Preparing for Takeoff”. Stratasy. <https://www.stratasy.com/es/resources/search/case-studies/bell-helicopter> (access: 8/4/2019).
- [43] “3D Printing a Space Vehicle”. Stratasy. <https://www.stratasy.com/es/resources/search/case-studies/nasa?phrase=nasa> (access: 8/4/2019).

- [44] P. Rambabu, N. Eswara Prasad, V. Kutumbarao, R. Wanhill, *Aerospace Materials and Material Technologies*, Edición. Singapore: Springer, 2017.
- [45] “Aluminum 6061-T6; 6061-T651”. ASM Aerospace Specification Metals. <http://asm.matweb.com/search/SpecificMaterial.asp?bassnum=ma6061t6> (access: 18/3/2019).
- [46] E. Olakanmi, R. Cochrane, K. Dalgarno. “A review on selective laser sintering/melting (SLS/SLM) of aluminium alloy powders: Processing, microstructure, and properties”, *Progress in Materials Science*, vol. 74, pages 401-477, October 2015. [On line]. Available at: <https://doi.org/10.1016/j.pmatsci.2015.03.002>. Access: 19/3/2019.
- [47] S. Farah, D. Anderson, R. Langer. “Physical and mechanical properties of PLA, and their functions in widespread applications — A comprehensive review”, *Advanced Drug Delivery Reviews*, vol. 107, pages 367-392, December 2016. [On line]. Available at: <https://doi.org/10.1016/j.addr.2016.06.012>. Access: 18/3/2019.
- [48] “Ficha de datos técnicos PLA”. Version 3.011. Ultimaker. 2017
- [49] B.Stanford, P. Dunning. “Optimal Topology of Aircraft Rib and Spar Structures under Aeroelastic Loads”. NASA. <https://ntrs.nasa.gov/search.jsp?R=20140007307> (access: 15/3/2019).
- [50] S. Khan, M. Awan. “A generative design technique for exploring shape variations”, *Advance Engineering Informatics*, vol. 38, Pages 712-724, October 2018. [On line]. Available at: <https://doi.org/10.1016/j.aei.2018.10.005>. Access: 17/3/2019.
- [51] “Generative Design” Siemens. <https://www.plm.automation.siemens.com/global/es/our-story/glossary/generative-design/27063> (access: 19/3/2019).
- [52] Pilots test. <https://pilotstest.com/test/quiz.php?quizgroup=1&id=2263> (access: 7/6/2019).
- [53] F. Sauer. “Aircraft Structural Considerations”. Vought Aircraft Industries. <http://aeweb.tamu.edu/aero214/Aircraft%20Structural%20Considerations%20Fall%202008.pdf> (access: 26/2/2019).
- [54] R. Roedts, R. Somero, C. Waskiewicz. “Airbus A380 Analysis”. Department of aerospace and ocean engineering, Virginia Tech. [http://www.dept.aoe.vt.edu/~mason/Mason\\_f/A380Roedts.pdf](http://www.dept.aoe.vt.edu/~mason/Mason_f/A380Roedts.pdf) (access: 24/2/2019).
- [55] D. Wallsworth. Twipu. <http://www.twipu.com/tag/BA2Airbus> (access: 7/6/2019).

- [56] “Kit de montaje impresora original 3D Prusa i3 mk2s”. Prusa 3D. <https://www.prusa3d.es/original-prusa-i3-3d-printer-kit-from-josef-prusa/#> (access: 10/5/2019).
- [57] “Prusa i3 mk2s”. 3Dhubs. [https://www.3dhubs.com/s3fs-public/original\\_prusai3mk2\\_0.png](https://www.3dhubs.com/s3fs-public/original_prusai3mk2_0.png) (access: 10/5/2019).
- [58] “PLA Easy Go”. BQ. <https://www.bq.com/es/pla> (access: 10/5/2019).
- [59] “PLA Easy Go filamento 1,75mm 1kg”. BQ. <https://store.bq.com/es/bobina-pla-easy-go-bq> (access: 10/5/2019).
- [60] J. Long. “Application Spotlight: Aerospace Wing Rib”. In-House solutions. <https://www.inhousesolutions.com/2016/11/application-spotlight-aerospace-wing-rib/> (access: 3/1/2019).
- [61] “Retours d'expérience industriels”. CENIS AFNET. [cnis.afnet.fr](http://cnis.afnet.fr) (access: 10/6/2019).
- [62] M. Baumann. “Raw material pricing and Additive Manufacturing”. 3D printing materials conference. [http://www.3dprintingmaterialsconference.com/wp-content/uploads/2014/06/MB\\_Raw\\_Materials\\_3.pdf](http://www.3dprintingmaterialsconference.com/wp-content/uploads/2014/06/MB_Raw_Materials_3.pdf) (access: 10/6/2019).
- [63] “Aluminio 6061 T6”. Made in China. [https://es.made-in-china.com/co\\_hlaluminum/product\\_Aluminum-Alloy-6061-T6-Price\\_einuoiygg.html](https://es.made-in-china.com/co_hlaluminum/product_Aluminum-Alloy-6061-T6-Price_einuoiygg.html) (access: 10/6/2019).
- [64] *Specification for additive manufacturing file format (AMF) Version 1.2*, AENOR UNE-EN ISO/ASTM 52915:2016
- [65] *Additive manufacturing. General principles. Part 2: Overview of processes and feedstock*, AENOR UNE-EN ISO 17296-2:2015
- [66] *Additive manufacturing. General principles. Part 3: Main characteristics and corresponding test methods*, AENOR UNE-EN ISO 17296-3:2014
- [67] *Additive manufacturing. General principles. Part 4: Overview of data processing*, AENOR UNE-EN ISO 17296-4:2014
- [68] *Plastics. Determination of flexural properties*, AENOR UNE-EN ISO 178:2010
- [69] “Ultimaker 2+ Specifications”. Ultimaker. <https://ultimaker.com/en/products/ultimaker-2-plus/specifications> (access: 3/6/2019).
- [70] “Asus X555LJ-XX036T”. PCcomponentes.

<https://www.pccomponentes.com/asus-x555lj-xx036t-intel-i7-5500u-8gb-1tb-gt920m-156> (access: 3/6/2019).

[71] “Sandisk Extreme SDHC 32GB”. PCcomponentes. <https://www.pccomponentes.com/sandisk-extreme-sdhc-32gb-clase-10> (access: 3/6/2019).

[72] “Equipos de protección”. Leroy Merlin. [http://www.leroymerlin.es/productos/herramientas/equipos\\_de\\_proteccion.html](http://www.leroymerlin.es/productos/herramientas/equipos_de_proteccion.html) (access: 3/6/2019).

[73] “Solid Edge”. Siemens. <https://www.plm.automation.siemens.com/store/es-es/solid-edge/?stc=usdf201336> (access: 3/6/2019).

[74] “Microsoft Office”. Fnac. <https://www.fnac.es/software/Microsoft-Office/s7738> (access: 3/6/2019).

[75] “Precio medio de la electricidad”. Lucera. <https://lucera.es/blog/precio-medio-electricidad-2018> (access: 3/6/2019).

[76] “Salarios para empleos de Ingeniero mecánico en España”. Indeed. <https://www.indeed.es/salaries/Ingeniero-mec%C3%A1nico-Salaries> (access: 3/6/2019).



## ANEXO 1

**Table A.1. NASA SC(2)-0610 Airfoil coordinates**

Parte de arriba		Parte de abajo	
X	Y	X	Y
0.000000	0.000000	0.000000	0.000000
0.002000	0.007600	0.002000	-0.007600
0.005000	0.011600	0.005000	-0.011600
0.010000	0.015500	0.010000	-0.015500
0.020000	0.020600	0.020000	-0.020600
0.030000	0.024100	0.030000	-0.024100
0.040000	0.026800	0.040000	-0.026800
0.050000	0.029000	0.050000	-0.029000
0.060000	0.030900	0.060000	-0.030900
0.070000	0.032600	0.070000	-0.032600
0.080000	0.034100	0.080000	-0.034100
0.090000	0.035500	0.090000	-0.035500
0.100000	0.036700	0.100000	-0.036700
0.110000	0.037800	0.110000	-0.037900
0.120000	0.038900	0.120000	-0.039000
0.130000	0.039900	0.130000	-0.040000
0.140000	0.040800	0.140000	-0.040900
0.150000	0.041700	0.150000	-0.041800
0.160000	0.042500	0.160000	-0.042600
0.170000	0.043200	0.170000	-0.043300
0.180000	0.043900	0.180000	-0.044000
0.190000	0.044500	0.190000	-0.044600
0.200000	0.045100	0.200000	-0.045200
0.210000	0.045600	0.210000	-0.045800
0.220000	0.046100	0.220000	-0.046300
0.230000	0.046600	0.230000	-0.046800
0.240000	0.047000	0.240000	-0.047200
0.250000	0.047400	0.250000	-0.047600
0.260000	0.047800	0.260000	-0.048000
0.270000	0.048100	0.270000	-0.048300
0.280000	0.048400	0.280000	-0.048600
0.290000	0.048700	0.290000	-0.048900
0.300000	0.048900	0.300000	-0.049100
0.310000	0.049100	0.310000	-0.049300
0.320000	0.049300	0.320000	-0.049500
0.330000	0.049500	0.330000	-0.049600
0.340000	0.049600	0.340000	-0.049700
0.350000	0.049700	0.350000	-0.049800



Manufacturing process optimization of an airplane wing rib by using additive manufacturing

0.360000	0.049800	0.360000	-0.049800
0.370000	0.049900	0.370000	-0.049800
0.380000	0.050000	0.380000	-0.049800
0.390000	0.050000	0.390000	-0.049700
0.400000	0.050000	0.400000	-0.049600
0.410000	0.050000	0.410000	-0.049500
0.420000	0.050000	0.420000	-0.049300
0.430000	0.049900	0.430000	-0.049100
0.440000	0.049800	0.440000	-0.048900
0.450000	0.049700	0.450000	-0.048600
0.460000	0.049600	0.460000	-0.048300
0.470000	0.049400	0.470000	-0.047900
0.480000	0.049200	0.480000	-0.047500
0.490000	0.049000	0.490000	-0.047000
0.500000	0.048800	0.500000	-0.046500
0.510000	0.048600	0.510000	-0.045900
0.520000	0.048300	0.520000	-0.045300
0.530000	0.048000	0.530000	-0.044600
0.540000	0.047700	0.540000	-0.043900
0.550000	0.047400	0.550000	-0.043100
0.560000	0.047000	0.560000	-0.042200
0.570000	0.046600	0.570000	-0.041200
0.580000	0.046200	0.580000	-0.040100
0.590000	0.045800	0.590000	-0.039000
0.600000	0.045300	0.600000	-0.037800
0.610000	0.044800	0.610000	-0.036600
0.620000	0.044300	0.620000	-0.035300
0.630000	0.043800	0.630000	-0.034000
0.640000	0.043200	0.640000	-0.032700
0.650000	0.042600	0.650000	-0.031300
0.660000	0.041900	0.660000	-0.029900
0.670000	0.041200	0.670000	-0.028400
0.680000	0.040500	0.680000	-0.026900
0.690000	0.039700	0.690000	-0.025400
0.700000	0.038900	0.700000	-0.023800
0.710000	0.038100	0.710000	-0.022200
0.720000	0.037200	0.720000	-0.020600
0.730000	0.036300	0.730000	-0.019000
0.740000	0.035300	0.740000	-0.017400
0.750000	0.034300	0.750000	-0.015800
0.760000	0.033200	0.760000	-0.014200
0.770000	0.032100	0.770000	-0.012600
0.780000	0.030900	0.780000	-0.011100
0.790000	0.029700	0.790000	-0.009600
0.800000	0.028500	0.800000	-0.008100

Manufacturing process optimization of an airplane wing rib by using additive manufacturing

0.810000	0.027200	0.810000	-0.006800
0.820000	0.025900	0.820000	-0.005600
0.830000	0.024500	0.830000	-0.004500
0.840000	0.023100	0.840000	-0.003500
0.850000	0.021600	0.850000	-0.002600
0.860000	0.020100	0.860000	-0.001800
0.870000	0.018500	0.870000	-0.001200
0.880000	0.016900	0.880000	-0.000700
0.890000	0.015300	0.890000	-0.000400
0.900000	0.013600	0.900000	-0.000300
0.910000	0.011900	0.910000	-0.000400
0.920000	0.010100	0.920000	-0.000700
0.930000	0.008300	0.930000	-0.001200
0.940000	0.006400	0.940000	-0.002000
0.950000	0.004500	0.950000	-0.003000
0.960000	0.002500	0.960000	-0.004200
0.970000	0.000400	0.970000	-0.005600
0.980000	-0.001800	0.980000	-0.007300
0.990000	-0.004200	0.990000	-0.009300
1.000000	-0.006700	1.000000	-0.011600